

CHEMISTRY

A European Journal

A Journal of



Accepted Article

Title: Triazolylidene iridium complexes with a pending pyridyl group for cooperative metal-ligand induced catalytic dehydrogenation of amines

Authors: Marta Valencia, Ana Pereira, Helge Müller-Bunz, Tomas R Belderrain, Pedro J Perez, and Martin Albrecht

This manuscript has been accepted after peer review and appears as an Accepted Article online prior to editing, proofing, and formal publication of the final Version of Record (VoR). This work is currently citable by using the Digital Object Identifier (DOI) given below. The VoR will be published online in Early View as soon as possible and may be different to this Accepted Article as a result of editing. Readers should obtain the VoR from the journal website shown below when it is published to ensure accuracy of information. The authors are responsible for the content of this Accepted Article.

To be cited as: *Chem. Eur. J.* 10.1002/chem.201700676

Link to VoR: <http://dx.doi.org/10.1002/chem.201700676>

Supported by
ACES

WILEY-VCH

Triazolylidene iridium complexes with a pending pyridyl group for cooperative metal-ligand induced catalytic dehydrogenation of amines

Marta Valencia,^{a,b} Ana Pereira,^{b,c} Helge Müller-Bunz,^b Tomás R. Belderráin,^c Pedro J. Pérez,^c Martin Albrecht*^{a,b}

^a *Department of Chemistry and Biochemistry, University of Bern, Freiestrasse 3, CH-3012 Bern, Switzerland. E-mail: martin.albrecht@dcb.unibe.ch*

^b *School of Chemistry, University College Dublin, Belfield, Dublin 4, Ireland*

^c *Laboratorio de Catálisis Homogénea, Unidad Asociada al CSIC, CIQSO- Centro de Investigación en Química Sostenible and Departamento de Química. Universidad de Huelva. 21007 Huelva (Spain)*

Abstract

Two iridium(III) complexes containing a *C,N*-bidentate pyridyl-triazolylidene ligand were prepared that are structurally very similar but differ in their pending substituent. While complex **1** contains a non-coordinating pyridyl unit, complex **2** has a phenyl group as triazolylidene substituent. The presence of the basic pyridyl unit has distinct effects on the catalytic activity of the complex in the oxidative dehydrogenation of benzylic amines, inducing generally higher rates, higher selectivity towards formation of imines vs secondary amines, and notable quantities of tertiary amines when compared to the phenyl-functionalized analogue. The role of the pyridyl functionality has been elucidated in a set of stoichiometric experiments, which demonstrate hydrogen bonding between the pending pyridyl unit and the amine protons of the substrate. Such $N_{\text{pyr}} \cdots H-N$ interactions are demonstrated by X-ray diffraction analysis, ^1H NMR and IR spectroscopy and suggest a pathway of substrate bond activation that involves concerted substrate binding through the Lewis acidic iridium center and the Lewis basic pyridyl site appended to the triazolylidene ligand, in agreement with ligand-metal cooperative substrate activation.

Introduction

Secondary amines and imines are valuable reactive intermediates with wide use for the synthesis of pharmaceutical and biological compounds, as well as industrially employed chemicals.^[1] Typically, the synthesis of secondary amines is accomplished by condensation of a primary amine with a suitable carbonyl compound, followed by imine reduction. Although amine alkylation with alcohols has received much attention in recent years,^[2,3] amine dehydrogenation is much less developed.^[4,5,6,7] In most cases, self-condensation of amines is carried out in the presence of heterogeneous catalytic metallic systems, such as gold or palladium, and in the presence of an oxidant, *e.g.* CeO₂ or O₂.^[8] Only a few examples are known in the literature where homogeneous noble metal catalysts have been used in amine cross-coupling reaction, mainly with ruthenium and iridium. These reactions normally require high temperature or the presence of an additive such as a base.^[9]

Key steps in amine dehydrogenation and coupling are the activation of the substrate N–H bond and the subsequent β hydrogen elimination to form the dehydrogenated imine intermediate. While the latter is a classic reaction trajectory brought about by transition metals,^[10] the N–H bond activation is typically imparted by Lewis bases. Hence, a plausible catalyst design entails a metal center with a labile ligand and a Lewis basic site in close mutual proximity, yet sterically constrained to avoid formation of a stable Lewis acid-base pair. This concept of frustrated Lewis pairs (FLPs) has been widely exploited with main group metals for the activation of dihydrogen and other substrates,^[11] and is conceptually related with metal-ligand bifunctionality.^[12]

Here we have designed a triazolylidene ligand that upon metal coordination forms a complex comprised of a chelate-stabilized late transition metal for dehydrogenation, and a pending pyridyl unit for N–H bond activation through hydrogen bonding. The underlying concept of this design is the strain imposed by the central five-membered heterocycle, which arranges the two pyridyl units in a wide angle that allows only one pyridyl unit to bind to the metal center. While in a monodentate triazolylidene complex, the metal carbene bond is dissecting the carbene N–C–C angle essentially evenly ($\theta = 0^\circ$, **A** in Fig. 1) metal chelation of pyridyl-triazolylidene ligands induces a large yaw angle (θ around 18°),^[13] which places the metal center far away from the second pyridyl unit (**B** in Fig 1). The yaw angle of this ligand is bigger than that observed in chelating bisimidazolylidene complexes ($\theta < 14^\circ$ for palladium coordination),^[14] or in a chelating bispyridyl-imidazolylidene complex ($\theta = 13.5^\circ$).^[15] The large yaw angle of the pyridyl-triazolylidene system **B**^[13,16] is therefore expected to prevent

coordination of the second pyridyl site,^[17] and to provide a basic entity for N–H activation in close proximity to the reactive metal center, while the metal coordinated to the triazolylidene can complete the dehydrogenation process via hydrogen elimination. Triazolylidenes,^[18] a subclass of N-heterocyclic carbenes (NHCs),^[19] have shown excellent catalytic activity in oxidative transformations such as water oxidation,^[20] alcohol dehydrogenation,^[9e,16d,f,21] and CH bond activation.^[22]

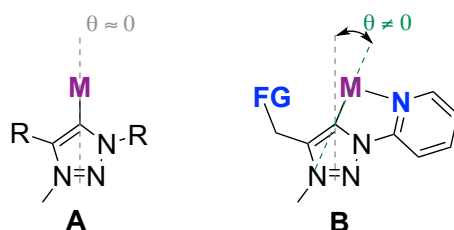
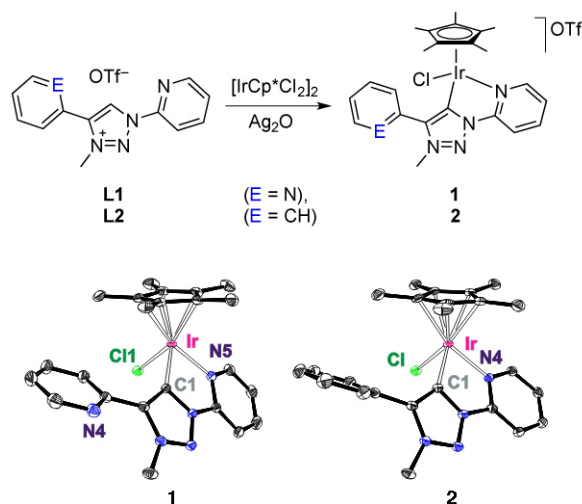


Figure 1. Schematic illustration of the position of the metal center in monodentate triazolylidene complexes (A) and in C,N-bidentate chelating systems (B), and the difference in yaw angle θ .

Results and Discussion

1. Synthesis of triazolium salts and triazolylidene iridium(III) complexes.

Based on our previous experience in chelating triazolylidene iridium complexes^[16,20] and in order to design this new type of functionalized triazolylidene ligand we have chosen as starting point the bis(pyridyl)triazolium salt **L1**, to study the capacity of a free pyridyl unit to cooperate actively in a catalytic process. The analogous ligand precursor **L2** lacks the second, potentially non-coordinating pyridyl functionality (Scheme 1) and will serve as model to evaluate the relevance of the pending pyridyl functionality. These two ligand precursors were prepared by methylation of the corresponding pyridyl-triazole compound with 1.2 equiv. of MeOTf.^[23] Precursor **L2** was obtained in excellent yield (96%), while methylation of the bis(pyridyl)triazole was less selective and therefore, **L1** with exclusively methylated triazolium salt and non-methylated pyridine groups was isolated in a moderate 28% yield after purification. Both salts displayed a characteristic low-field CH_{trz} proton singlet in the ^1H NMR spectra (δ_{H} 9.68 and 9.04 for **L1** and **L2**, respectively, CDCl_3 solution).



Scheme 1. Synthesis of iridium complexes **1** and **2** and ORTEP representation of both complexes (50% probability level; hydrogen atoms, solvent molecules, non-coordinated OTf⁻ anions, and the second independent molecule in the unit cell of **1** omitted for clarity).

The synthesis of the triazolylidene iridium(III) complexes **1** and **2** was carried out *via* Ag₂O-mediated proton abstraction and *in situ* transmetallation with [Ir(Cp*)Cl₂]₂ in a one pot procedure (Scheme 1). Complexes **1** and **2** are air stable yellow solids, which were conveniently purified by column chromatography and isolated in 96% and 95% yield, respectively.^[24] Both were characterized by elemental analysis, ¹H and ¹³C{¹H} NMR spectroscopy and X-ray diffraction analysis. We note that the synthesis of complex **1** was highly chemoselective and chelation only involved the electron-rich pyridyl group linked to the the triazolylidene nitrogen^[16b] as indicated by spectroscopic analysis of a sample from the crude reaction mixture. Metalation of the triazole heterocycle was indicated by the disappearance of the low-field CH_{trz} proton resonance of the ligand precursors in the ¹H NMR spectra. Additionally, the spectrum of complex **1** showed two sets of four aromatic proton resonances, indicating the presence of two inequivalent pyridyl units and hence a single isomer. The set of four aromatic proton resonances of the chelating pyridyl group in complex **1** appears at almost identical frequency as those of complex **2**. Unambiguous assignment of the pyridyl protons in complex **1** was accomplished by ¹H–¹H correlation spectroscopy, and by establishing Nuclear Overhauser Effects between the pyridyl C³–H proton of the non-metalated pyridyl unit (δ_H 8.06) and the triazolylidene N–CH₃ group (δ_H 4.49). The ¹³C NMR spectra showed the carbene carbon resonance at 153.3 and 151.8 ppm for complex **1** and **2** respectively. The carbene chemical shifts together with the aromatic carbon resonances of the Cp* ligand at 91.9 and 91.7 ppm for

complexes **1** and **2**, respectively, suggest that the Lewis acid character of these iridium metal centers is similar.

Complexes **1** and **2** were crystallized by slow diffusion of Et₂O into a solution of the complex in CH₂Cl₂. Both complexes adopt a three-legged piano-stool-type molecular geometry, comprised of a *N,C*-bidentate chelating pyridyl-triazolylidene ligand, while the second pyridyl moiety in **1** is non-coordinating. Selective bonding of the more electron-rich pyridyl ring attached to the triazolylidene nitrogen as surmised from solution analysis is therefore confirmed in the solid state. Such behavior was previously observed in cyclometalation reactions when two phenyl substituents were present as triazolylidene wingtip groups, and C–H bond activation exclusively involved the more electron-rich N-bound phenyl group.^[16b] The metal environment is very similar in complexes **1** and **2** and bond lengths and angles are essentially identical and within the expected range.^[19e] The yaw angle in complexes **1** and **2** is also identical ($\theta = 15.4^\circ$). The pendant pyridyl group in complex **1** features the nitrogen in pseudo *anti* orientation to the iridium center, presumably due to electrostatic repulsion of the nitrogen lone pair and the electron density at the iridium-bound chloride.

Table 1. Selected bond lengths (Å) and angles (°) for complexes **1** and **2**.

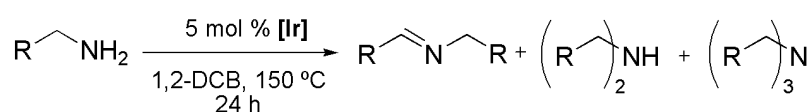
| | 1 | 2 |
|---|-----------|-----------|
| Ir–C _{trz} | 2.024(2) | 2.023(2) |
| Ir–N _{pyridyl} | 2.127(2) | 2.129(2) |
| Ir–Cl | 2.4079(7) | 2.3904(6) |
| C _{trz} –Ir–N _{pyridyl} | 77.36(8) | 77.28(8) |
| Cl–Ir–C _{trz} | 88.14(6) | 85.88(6) |
| Cl–Ir–N _{pyridyl} | 85.27(5) | 87.62(5) |
| N _{trz} –C _{trz} –M | 113.7(1) | 113.8(6) |
| C _{trz} –C _{trz} –M | 144.4(2) | 118.4(1) |
| θ | 15.4 | 15.4 |

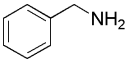
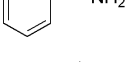
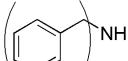
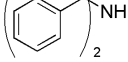
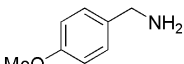
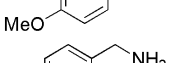
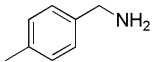
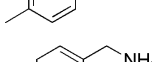
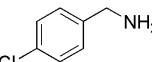
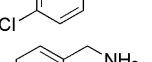
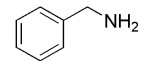
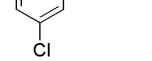
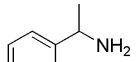
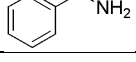
2. Catalytic Experiments with protic substrates.

The activity of related triazolylidene iridium complexes as catalyst precursors for the oxidation of oxygen-containing protic substrates such as H₂O or alcohols^[20,21] prompted us to investigate the ability of complexes **1** and **2** to catalyze the related dehydrogenation of amines. In particular we aimed at probing the bifunctional character of the triazolylidene iridium system **1** due to the presence of a basic pyridyl group as compared to the inert phenyl substituent in complex **2**.

The dehydrogenation of benzylamine and related substrates was evaluated with complexes **1** and **2** under conditions similar to those reported for the oxidation of alcohols with related monofunctional triazolylidene complexes, *i.e.* catalyst loading of 5 mol% in 1,2-dichlorobenzene at 150 °C and in the absence of an oxidant or a base.^[16,21,25] Under these conditions, both complexes **1** and **2** are active catalysts and converted primary amines into a mixture of secondary imines, secondary amines, and tertiary amines in different proportions. The results of the catalytic experiments are compiled in Table 2.

Table 2. Oxidative coupling of amines^a



| Entry | Cat | Amine | Conversion (%) ^b | Imine ^c | 2° Amine ^c | 3° Amine ^c |
|-------|----------|---|-----------------------------|--------------------|-----------------------|-----------------------|
| 1 | 1 |  | 97 | 65 | 31 | 4 |
| 2 | 2 |  | 93 | 52 | 47 | 1 |
| 3 | 1 |  | 57 | 28 | 43 ^d | 29 |
| 4 | 2 |  | 40 | 21 | 60 ^d | 19 |
| 5 | 1 |  | 95 | 50 | 28 | 22 |
| 6 | 2 |  | 97 | 55 | 21 | 4 |
| 7 | 1 |  | 95 | 63 | 26 | 11 |
| 8 | 2 |  | 96 | 53 | 35 | 12 |
| 9 | 1 |  | 93 | 70 | 29 | 0 |
| 10 | 2 |  | 76 | 55 | 45 | 0 |
| 11 | 1 |  | 95 | 86 | 13 | 1 |
| 12 | 2 |  | 65 | 68 | 32 | 0 |
| 13 | 1 |  | 80 | 42 | 57 | 0 |
| 14 | 2 |  | 80 | 44 | 56 | 0 |

[a] Conditions: amine (0.2 mmol), [Ir] (5 mol% of catalyst), 1,2-dichlorobenzene (1,2-DCB; 2 mL), 150 °C. [b] Determined by ¹H NMR spectroscopic analysis with hexamethylbenzene as internal standard. [c] Ratio of products given in percentage. [d] Secondary amine as substrate.

Both complexes **1** and **2** produce a catalytically active species that reaches excellent conversions after 24 h. Analysis of the products showed a mixture comprised of the benzylidene imine, dibenzylamine, and tribenzylamine (entries 1, 2). The latter was observed only in traces in catalytic runs with **2** (ca. 1%), and was a bit more pronounced when the pyridyl-containing complex **1** was used as precursor. The ratio of imine vs secondary amine was about 2:1 when starting with complex **1**, while it was close to 1:1 with the phenyl-substituted triazolylidene

iridium complex **2**. The enhanced selectivity of complex **1** towards imine formation suggests that H₂ is not captured in the metal coordination sphere, therefore hampering hydrogenation of the imine to the secondary amine. In contrast, complex **2** is more efficient in storing hydrogen and in re-hydrogenating the substrate in what is often referred to as a “borrowing hydrogen” process.^[7,26] The low selectivity observed for complexes **1** and **2** contrasts previous work with related triazolylidene ruthenium complexes and iridium imidazolylidene complexes,^[9b,e] which afforded imine products selectively. Accordingly, both complexes **1** and **2** are better re-hydrogenation catalysts than the previously investigated systems.

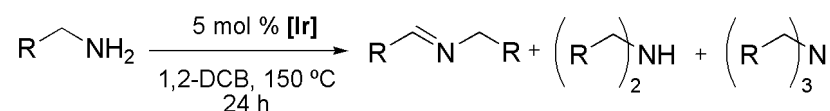
The formation of tertiary amines indicates that the dehydrogenated benzylimine is activated, since secondary amines are not usually forming tertiary amines easily. However, tertiary amines were reported to be formed from N-methylaniline and benzylalcohol.^[9b] Hence, it is conceivable that the tertiary amines observed with complex **1** are formed via the formation of benzaldehyde from benzylimine in the presence of fortuitous water. In order to further investigate the reactivity of the secondary amine, dibenzylamine was used as a substrate for dehydrogenation (entries 3,4). With complex **1** under standard reaction conditions, indeed nearly 30% tribenzyl amine was obtained, and about equal amounts of dehydrogenated imine. The conversion was lower with complex **2**, suggesting that the pyridyl group had a moderately rate-enhancing effect.

The trends deduced from benzylamine conversion were also observed with different substrates (Table 2, entries 5–14). Generally, the pyridyl group in complex **1** induces a slightly higher catalytic dehydrogenation activity than the phenyl group in complex **2**. With activating electron-donating methoxy groups as aromatic substituents on the substrate, the higher activity resulted in substantially higher ratios of tertiary amine products (entries 5,6). The same trend, albeit weaker, was also observed with less donating methyl substituents (entries 7,8). When the substrate contains electron-withdrawing chloro-substituents, only complex **1** induced full conversion while the catalyst precursor lacking the pyridyl unit gave only about 70% conversion within 24 h (entries 9–12). In addition to the enhanced activity, in all cases the imine to secondary amine ratio is higher with complex **1** than with complex **2**.

To further probe the relevance of the hydrogen borrowing process, catalytic studies were carried out under inert conditions in a Young NMR tube in the presence of complex **1**, and under strict control of the atmosphere (Table 3). When focusing on modifications after full substrate conversion, we note that hydrogen transfer continues. Thus, while no primary amine was observed anymore in the reaction mixture after 24 h (entry 1), prolonging the reaction for a

further 24 h continued to induce dehydrogenation of the secondary amine and increased the ratio of both the imine and the tertiary amine (entry 2). These secondary dehydrogenation processes are not dependent on the presence of oxygen from the air, and similar transformations were also observed when the reaction mixture was degassed and kept under an argon atmosphere for the second 24 h (entries 3–5). However, when the atmosphere after 24 h is changed to H₂, rapid hydrogenation of the imine took place (entries 6,7). Therefore, these experiments identify complex **1** as a highly active catalyst precursor for imine hydrogenation under a reducing atmosphere. Interestingly, the slow formation of the tertiary amine is not suppressed by a H₂ atmosphere, indicating that dehydrogenation of the secondary amine is still occurring, though the equilibrium is shifted from the imine to the amine side.

Table 3. Oxidative coupling of benzylamine under different conditions ^a

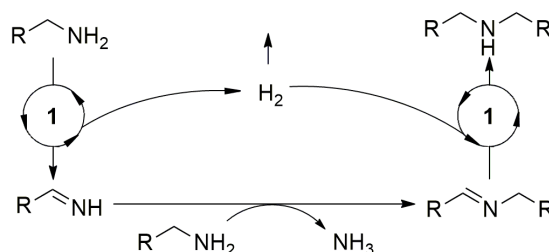


| Entry | conversion (%) ^c | gas | time | Ph-CH=NR ^b | HNR ₂ ^b | NR ₃ ^b | comment |
|-------|-----------------------------|----------------|------|-----------------------|-------------------------------|------------------------------|-------------------------------|
| 1 | 94 | Air | 24 h | 46 | 54 | 0 | 0.5 mL (NMR tube) |
| 2 | 98 | Air | 48h | 63 | 32 | 5 | 0.5 mL (NMR tube) |
| 3 | 95 | Air | 24 h | 61 | 38 | 1 | 2 mL (closed vial) |
| 4 | 95 | Ar | 26 h | 60 | 37 | 3 | c) |
| 5 | 96 | Ar | 48 h | 59 | 25 | 17 | c) |
| 6 | 94 | H ₂ | 26 h | 7 | 89 | 4 | c) |
| 7 | 96 | H ₂ | 48 h | 1 | 84 | 15 | c) |
| 8 | 62 | Air | 24 h | 54 | 46 | 0 | 1 mL (vial with no headspace) |

[a] Conditions: benzylamine (0.1 mM in 1,2-dichlorobenzene), **1** (5 mol%), 150 °C, conversion of benzylamine, determined by ¹H NMR spectroscopic analysis with hexamethylbenzene as internal standard; b) relative product ratio in %; c) 0.5 mL product mixture from entry 3 was transferred to a pressure NMR tube and charged with the indicated gas after 0 h and after 2 h times reported are cumulated (e.g entry 4 is 24 h as in entry 3 plus 2 h under Ar).

The formation of amine and imine products observed in the absence of a hydrogen atmosphere was consequently attributed to a partial degassing and loss of H₂ from the reaction mixture. Accordingly, the H₂ formed in the first step of the reaction during dehydrogenation of the substrate is not stored in the metal coordination sphere but more likely as H₂ in solution. Attempts to detect H₂ by NMR spectroscopy were prevented by the small quantities of H₂

formed and by the high reaction temperature which was used for the reaction. In agreement with this model, a catalytic run in a closed vial without any headspace gave only incomplete conversion after 24 h (62% vs 95% under standard conditions) and shifted the product selectivity towards the secondary amine (imine/amine ratio from 2:1 to 1:1 entry 8). The reduced catalytic turnover suggests that dehydrogenation of the substrate amine is disfavored, in agreement with a hydrogen borrowing mechanism (Scheme 2). Accordingly, the release of H₂ to the atmosphere enhances the rate of dehydrogenation as the initial step. Moreover, the selectivity change is commensurate with complex **1** being a catalyst for the hydrogenation of imines when hydrogen is forced to remain in the reaction mixture (last step), as induced by the increase of H₂ in solution when the headspace is minimized.



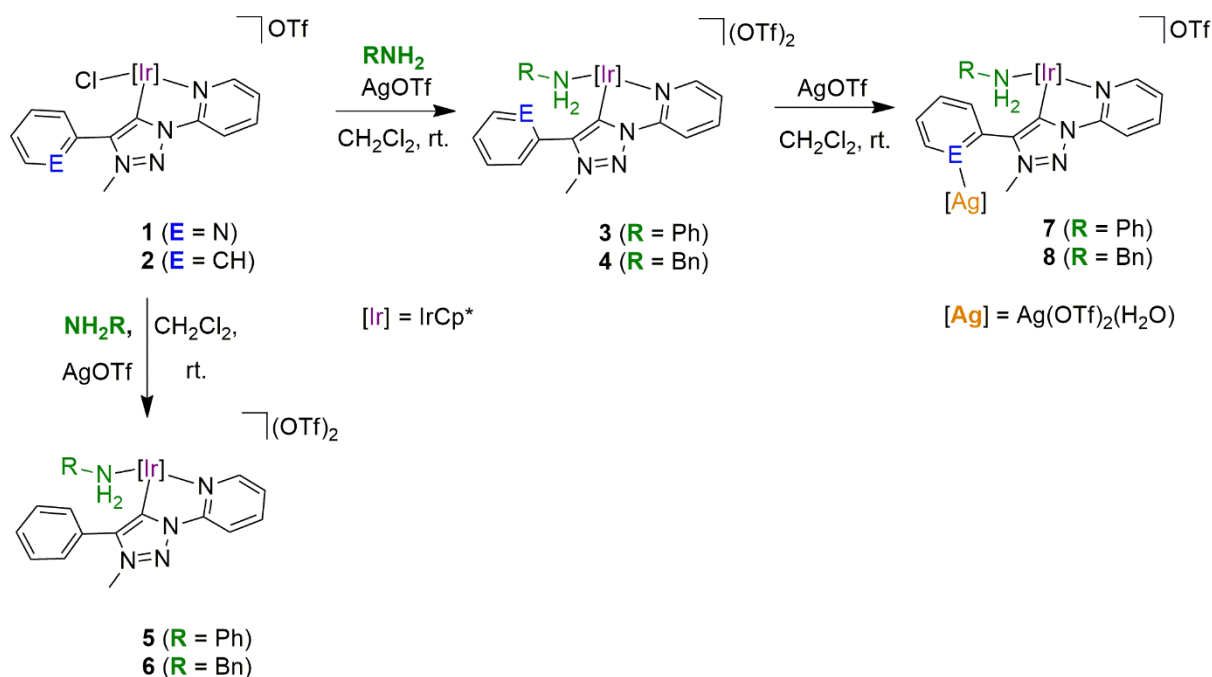
Scheme 2. Amine alkylation by proton borrowing reaction.

Hydrogen borrowing is a widely accepted process in the homo-coupling of amines to imines and subsequent reduction of the imine intermediates to secondary amines, leading to an overall alkylation of amines.^[27] Generally, a metal hydride has been inferred as active species,^[9h,28] which removes an acidic proton from the substrate either via a metal-bound hydride to form H₂, or via another basic ligand site to store a H₂ equivalent within the catalytic structure. According to the selectivity patterns observed with complex **1**, storage of a H₂ equivalent is not supported in this case. Presumably, the basic pyridyl site in complex **1** assists the substrate deprotonation, which facilitates then H₂ release and hence a larger ratio of imine vs amine formation. Alternatively, we hypothesized that the pendant pyridyl group may be involved in substrate recognition and binding rather than proton abstraction. In order to explore such bonding in more detail, several stoichiometric experiments were carried out.

3. Stoichiometric Experiments

Substrate bonding was investigated by the reaction of complex **1** with one equivalent of amine, induced by chloride abstraction with stoichiometric amounts of AgOTf. To avoid dehydrogenation, these reactions were performed at room temperature, initially using aniline as a model substrate which has no β hydrogens and cannot dehydrogenate. Subsequently, benzylamine was used as a real substrate. These reactions afforded complexes **3** and **4** in high yields (87%) as air-stable, pale yellow solids (Scheme 3). For comparative purposes, complexes **5** and **6** were prepared. These complexes are analogues of **3** and **4**, respectively, yet lacking the pyridyl function and therefore allow the assessment the relevance of substrate recognition and potential hydrogen bonding. The relevance of complex **4** as a catalyst precursor was demonstrated by exposing this complex to benzylamine under catalytic conditions as described in Table 2. Similar yields and selectives as complex **1** were obtained (Table S6), yet initial activities were lower (Fig. S1).

When complexes **3** and **4** were treated with a second equivalent of AgOTf, the heterobimetallic Ir/Ag complexes **7** and **8** were formed, in which the pendant pyridyl is coordinated to the silver(I) center. Hence, complexes **3–6** provide insight into the role of the *hydrogen bond acceptor* (pyridyl vs phenyl pending group), while complexes **7** and **8** contain a modified Lewis acid coordinated to the pyridyl group and hence constitute a model with a modified ‘hydrogen bond’ *donor*. Comparison of the different bonding situations was performed in the solid state by X-ray diffraction, and in solution by NMR and IR spectroscopy.



Scheme 3

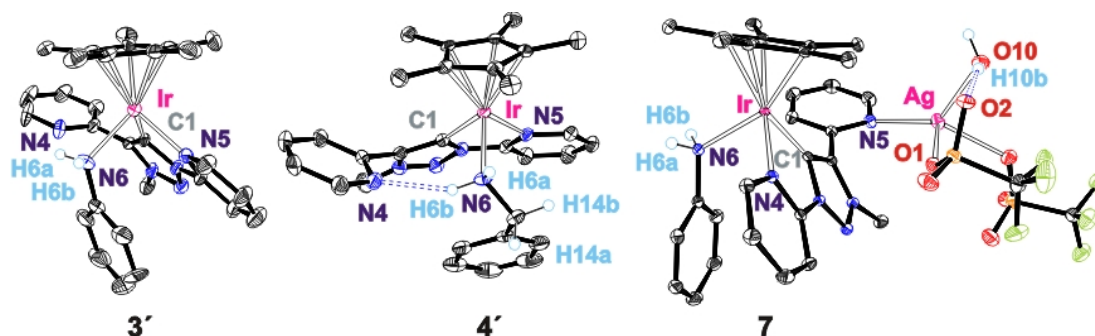


Figure 2. ORTEP representation of complexes **3'**, **4'** and **7** (50% probability level, most hydrogen atoms, solvent molecules, and non-coordinated OTf⁻ and BPh₄⁻ anions omitted for clarity).

Crystals suitable for X-ray diffraction analysis were obtained for complexes **3'**, **4'** and **7**. For **3** and **4**, counterion exchange from OTf⁻ to BPh₄⁻ was essential to grow crystals of sufficiently high quality. The molecular structures of all three complexes reveal the typical three-legged piano stool geometry around iridium (Figure 2).^[29] In addition, complex **7** features a silver(I) center in a distorted tetrahedral coordination geometry defined by two monodentate OTf ligands, a coordinated water molecule and the pyridyl group that was non-coordinating in complex **1**.

Bond lengths and angles around iridium are unsurprising and very similar to the metric data of complex **1** (Table 4). In all three complexes, the pyridyl group that is not bound to iridium is interacting with Lewis acids. In complex **3'**, the N_{aniline}-H...N_{pyr} distance is relatively long at 3.08 Å, suggesting only a weak hydrogen bond.^[30] The stabilizing nature of this interaction is supported by the orientation of the heterocyclic pyridyl nitrogen, which is pointing towards the amine proton, whereas an opposite orientation was observed in complex **1** (*vide supra*). In complex **4'** with a coordinated benzylamine ligand, the N_{Bn}-H...N_{pyr} distance is much shorter, 2.27(3) Å, indicative of a relatively strong intramolecular hydrogen bond. A strong interaction between the acidic amine proton and the basic pyridyl unit may also rationalize the slightly shorter Ir-C_{trz} bond in complex **4'** compared to complexes **3'** and **7**, 2.016(2) vs 2.043(5) and 2.037(2), respectively. No such NH...N interaction was observed in complex **7**, and instead, the pyridyl nitrogen is bound to the silver ion with a distance of 2.252(2) Å, coincidentally similar to the H...N distance in complex **4'**.

Table 4. Selected bond lengths (Å) and angles (in degrees) for complexes **3'**, **4'** and **7**.

| | 3' (X = H _{aniline}) | 4' (X = H _{amine}) | 7 (X = Ag) |
|-----------------------|---------------------------------------|-------------------------------------|-------------------|
| Ir-C _{trz} | 2.043(5) | 2.016(2) | 2.037(2) |
| Ir-N _{pyr} | 2.130(5) | 2.138(1) | 2.125(2) |
| Ir-N _{amine} | 2.043(5) | 2.147(2) | 2.191(2) |

| | | | |
|---|----------|----------|----------|
| C _{trz} -Ir-N _{pyr} | 76.6(2) | 76.28(7) | 77.75(9) |
| N _{amine} -Ir-C _{trz} | 87.1(2) | 86.87(7) | 91.30(9) |
| N _{amine} -Ir-N _{pyr} | 88.2(2) | 94.62(6) | 83.15(8) |
| N _{pyr} ...X | 3.082(4) | 2.27(3) | 2.252(2) |
| N _{trz} -C _{trz} -M | 113.8(3) | 115.3(1) | 113.2(2) |
| C _{trz} -C _{trz} -M | 142.9(4) | 142.0(2) | 145.5(2) |

Hydrogen bonding was also observed in solution by NMR and IR spectroscopy (CH₂Cl₂). For example in the ¹H NMR spectrum of complex **3**, the pyridyl C6-H resonance appears at δ_H = 9.06 (atom labeling scheme as in Fig. 3), at significantly lower field compared to the same resonance in complex **1** (δ_H = 8.73). Deshielding upon aniline coordination indicates a lower electron density in the heterocycle, which is expected upon Lewis acid bonding. Principally, a downfield shift may also be entailed by indirect coulombic effects, arising from chloride abstraction and the associated increase of the formal charge at the iridium center from monocationic in **1** to dicationic in **3**. However, comparison with the phenyl substituted systems (complex **2** vs. **5**) strongly supports the notion that such electrostatic considerations are not a dominant factor, as the phenyl proton resonances shift only marginally (<0.1 ppm) upon amine coordination. (*cf.* Δδ > 0.3 ppm with the pyridyl homologue). The chemical shift of the pyridyl C6-H proton does not vary upon exchange of the counterion from weakly coordinating OTf⁻ to less coordinating BPh₄⁻, suggesting that anion effects are not interfering with hydrogen bonding.

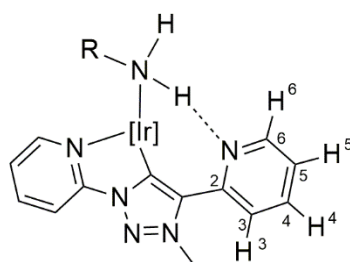


Figure 3. Carbon and hydrogen numbering scheme for the non-coordinated pyridyl unit in complexes **3** and **4** ([Ir] = [Ir(Cp*)²⁺]).

Benzylamine coordination and formation of complex **4** induced a similar shift as observed upon aniline bonding, with the diagnostic resonance of the pyridyl C6-H in complex **4** resonating at δ_H = 9.01. The downfield shift of this resonance is slightly more pronounced when the Lewis acid is exchanged from a benzylamine proton to a Ag⁺ ion, with δ_H = 9.09 and 9.08 in complexes **7** and **8**, respectively. Hence, the deshielding of this proton supports bonding of a Lewis acidic

site in all complexes **3**, **4**, **7**, and **8** and corroborates intramolecular hydrogen bonding in complexes **3** and **4** also in solution.

The resonances due to the NH₂ unit were not diagnostic in the aniline complexes **3**, **5**, and **7** and appeared as broad signals around $\delta_{\text{H}} \sim 7.5$ (Figure S3). A similar resonance pattern was observed at $\delta_{\text{H}} \sim 5.4$ for the benzylamine protons in complexes **6** and **8**, in which the benzylamine NH₂ unit is not hydrogen bonded either due to the lack of hydrogen bond acceptor (in **6**) or due to competition of a different Lewis acid (Ag⁺ in complex **8**; Figure 4). Complex **4** in contrast features two distinct resonances at $\delta_{\text{H}} = 5.5$ and 5.3 for the NH₂ protons. The diastereotopic nature of the two NH protons in complex **4** indicates a locked configuration at the amine nitrogen, in full agreement with hydrogen bonding in this complex.^[31]

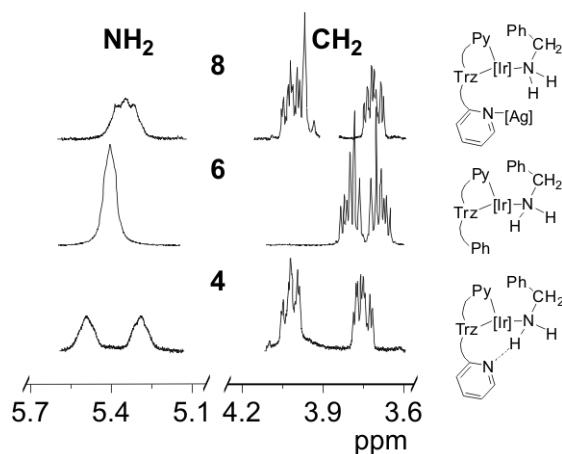


Figure 4. Section of the ¹H NMR spectrum (400 MHz, acetone-*d*₆, 298 K) of complexes **4**, **6** and **8** featuring the NH₂ and CH₂ proton resonances of the benzylamine ligand.

The ¹³C NMR spectra showed only minor differences upon amine coordination for the pyridyl unit and the Cp* ligand, generally to lower field (<2 ppm). For example, Cp* resonances shifted downfield from $\delta_{\text{C}} = 91.8(\pm 0.1)$ ppm in complexes **1** and **2** to $\delta_{\text{C}} = 93.4(\pm 0.1)$ ppm upon aniline coordination and to $\delta_{\text{C}} = 93.2(\pm 0.1)$ ppm upon benzylamine coordination, likely because the iridium metal center is formally dicationic in complexes **3–8** while it is monocationic in complexes **1** and **2**. Remarkably, the carbene resonance is insensitive to this change and appears at $\delta_{\text{C}} = 153.2(\pm 0.1)$ ppm in the pyridyl complexes **1**, **3**, and **7** containing an aniline ligand. The chemical shift is affected, however, by the type of amine; the C_{trz}–Ir resonance of the aniline complexes appears at lower field than that of the benzylamine complexes **4** and **8** ($\delta_{\text{C}} = 150.7$ ppm).

Hydrogen bonding was further investigated by IR spectroscopy of complexes **1–8** as the $N_{\text{amine}}H \dots N_{\text{pyr}}$ interactions are IR sensitive. Figure 5a shows superimposed spectra of the aniline complexes **3**, **5**, and **7** in the $4000\text{--}2000\text{ cm}^{-1}$ range. When comparing the spectrum of complex **3** with the spectra of amine-free complexes **1**, **2** and its deuterated analogue **3-D₂**, which was prepared by deuteration of the aniline protons of **3** in methanol-*d*₄, the strong absorptions at $\nu_{\text{NH}} = 3235$ and 3124 cm^{-1} for complexes **3**, **5** and **7** can unambiguously be assigned to the asymmetric and symmetric N–H stretching bands, respectively (Fig. 4a). Just slightly different energies were noted for the benzylamine series ($\nu_{\text{NH}} = 3233$ and 3150 cm^{-1} Fig. 5b). These bands are significantly lower than the N–H stretch vibrations of free aniline ($\nu_{\text{NH}} = 3429$ and 3352 cm^{-1})^[32] and its derivatives such as *p*-methylaniline or *m*-methylaniline,^[33] Likewise, the NH stretching vibrations of free benzylamine were reported at higher energy, $\nu_{\text{NH}} = 3372$ and 3303 cm^{-1} .^[34]

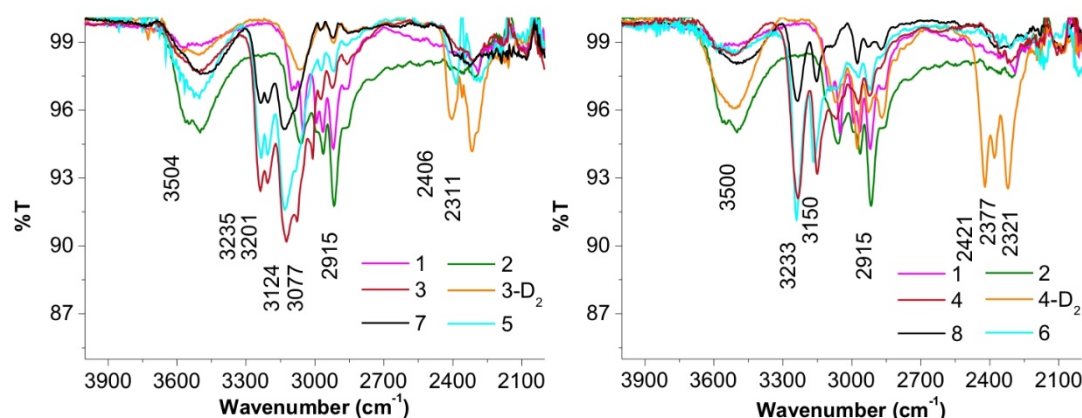


Figure 5. Infrared spectra of the complexes in the $4000\text{--}2000\text{ cm}^{-1}$ range; a) spectra of complexes **1**, **2**, **3**, **3-D₂**, **5** and **7** (aniline series); b) spectra of complexes **1**, **2**, **4**, **4-D₂**, **6**, and **8** (benzylamine series).

Upon metal coordination, the N–H stretch vibrations typically experience a bathochromic shift of around 100 cm^{-1} . Extensive vibrational studies with transition metals of the first row, cadmium, and mercury, confirmed this trend.^[32,35] For example aniline coordinated to copper features N–H vibrational bands at $\nu_{\text{NH}} = 3301$ and 3234 cm^{-1} .^[36] They vary by less than 10 cm^{-1} when using methylated or chelating aniline derivatives.^[33,37] Directly relevant to our studies, several iridium complexes containing a coordinated amine ligand were reported. For example, Bergman and coworkers assigned the bands at $\nu_{\text{NH}} = 3282$ and 3239 cm^{-1} to the N–H stretch of an Ir–NH₂*t*Bu complex, and $\nu_{\text{NH}} = 3266$ and 3197 cm^{-1} for an iridium complex containing a sterically hindered aniline ligand with *i*Pr substituents in *ortho* position.^[38] Similarly, Ikariya

and coworkers observed bands in the 3325–3045 cm^{-1} range for several amino iridium and ruthenium complexes,^[39] hence corroborating our assignments. In addition, the lower energy observed in our system is indicative for efficient hydrogen bonding.

The corresponding deuterated complex **3-D₂** shows the expected shift of these stretching modes to lower frequency (ν_{ND} around 2410 and 2315 cm^{-1}). The $\nu_{\text{NH}}/\nu_{\text{ND}}$ ratio is ideally 1.369 for free molecules,^[40] yet significantly lower in hydrogen-bonded systems.^[41] For example, this ratio drops to 1.355 for H_2O ,^[42] and as far as 0.96 for strongly hydrogen-bonding HCrO_2 .^[43] For complex **3**, the $\nu_{\text{NH}}/\nu_{\text{ND}}$ ratio is 1.34(1), which is smaller than the ratio measured in free aniline (1.36(2) for Ph-NH_2 vs Ph-ND_2) and also the ratio reported for water (see above), hence corroborating the presence of a moderate $\text{NH}\dots\text{N}$ hydrogen bond.^[40]

A similar evaluation of the benzylamine complex **4** ($\nu_{\text{NH}} = 3233$ and 3150 cm^{-1}) and its analogue containing a dideuterated benzylamine ligand **4-D₂** ($\nu_{\text{ND}} = 2400$ and 2320 cm^{-1}) gave a $\nu_{\text{NH}}/\nu_{\text{ND}}$ ratio of 1.35(1). An identical ratio was observed for the free benzylamine (Bn-NH_2 vs Bn-ND_2), which suggests a $\text{NH}\dots\text{N}_{\text{pyr}}$ hydrogen bond strength similar to that of the aniline complex **3**. While X-ray analysis and NMR spectroscopy indicate a stronger hydrogen bond interaction for the benzylamine complex **4** than for aniline, the IR analyses may be compromised by the relatively large error, presumably due to the broadness and splitting of the absorption bands.

Conclusions

We have developed a pair of triazolylidene iridium complexes that catalyze the oxidative coupling of benzylic amines under base- and oxidant-free conditions. In addition, these complexes are catalytically active both in the dehydrogenation of benzylic secondary amines and the inverse reaction, *i.e.* the hydrogenation of imines. Such dual reactivity may be of interest for amine racemization, *e.g.* for dynamic kinetic resolution, as well as for the reversible storage and release of dihydrogen. Activity and selectivity of the catalyst is affected by the availability of a pendant pyridyl site that can act as Lewis base for the stabilization of substrates through hydrogen bonding. Such metal-ligand cooperation for substrate conversion has been evidenced by a series of stoichiometric experiments. Optimization of these effects will be greatly facilitated by the synthetic versatility of the click reaction to generate the triazole ligand scaffold which allows to introduce a variety of functional groups. The confinement of a redox-active Lewis acidic metal site and a Lewis basic imine unit within an active site is reminiscent of the concept of frustrated Lewis pairs, and constitutes an appealing concept for the activation of

protic substrates and for designing new generations of catalysts for de- and re-hydrogenation of potential H₂ carriers. Further optimization will therefore include modifications in the ligand as well as the substrate to access an ideal Lewis acid base match.

Experimental Section

1-(2-pyridyl)-4-(2-pyridyl)triazole, 1-(2-pyridyl)-4-(2-phenyl)triazole,^[23] and [Cp*IrCl₂]₂ were prepared according to literature procedures.^[44] Solvents were dried by passage through solvent purification columns. All other reagents were purchased from commercial sources and used without further purification. All reactions involving iridium were carried out under strict exclusion of air using Schlenk-tube techniques under an atmosphere of dry nitrogen. All ¹H and ¹³C NMR spectra were recorded on Varian spectrometers operating at 400, 500 or 600 MHz (¹H NMR). Chemical shifts (δ) are given in ppm and referenced to residual solvent resonances. Signal assignments are based on heteronuclear correlation and heteronuclear multiple bond correlation experiments. Elemental analysis was performed by the microanalytical laboratories of University College Dublin and the University of Bern. FT-IR spectra were recorded on a Jasco FT-IR 4700 spectrometer with attenuated total reflectance (ATR) sampling technique at room temperature.

Synthesis of L1. A suspension of 1-(2-pyridyl)-4-(2-pyridyl)triazole (700 mg, 2.74 mmol) and MeOTf (361 μL, 3.29 mmol) in dry CH₂Cl₂ (15 mL) was stirred at 0 °C for 30 min and then at r.t for 2 h. The solvent was evaporated under reduced pressure. The residue was precipitated and washed with Et₂O. Analysis of the crude product by ¹H NMR spectroscopy showed a mixture of two products (triazolium vs pyridinium ca. 1:3). The crude mixture was purified by gradient flash chromatography (SiO₂, CH₂Cl₂/MeOH 40:1 to 20:1). L1 was eluted as the first fraction (white solid, 300 mg, 28%). ¹H NMR (CDCl₃, 400 MHz, 298 K): δ 9.68 (s, 1H, H_{trz}), 8.79 (d, J_{HH} = 4.8 Hz, 1H, H_{py}), 8.67 (dd, J_{HH} = 4.8, 0.9 Hz, 1H, H_{py}), 8.27 (d, J_{HH} = 8.0 Hz, 1H, H_{py}), 8.26 (d, J_{HH} = 7.7 Hz, 1H, H_{py}), 8.12 (td, J_{HH} = 8.0, 1.6 Hz, 1H, H_{py}), 8.01 (td, J_{HH} = 7.7, 1.5 Hz, 1H, H_{py}), 7.64 (dd, J_{HH} = 8.0, 4.8 Hz, 1H, H_{py}), 7.53 (dd, J_{HH} = 7.7, 4.8 Hz, 1H, H_{py}), 4.79 (s, 3H, NCH₃). ¹³C NMR (CDCl₃, 100.6 MHz, 298 K): δ 150.1, 149.6 (2 x CH_{arom}), 146.7, 142.8 (2 x C_{ipso}), 142.3 (C_{trz}), 140.6, 138.6, 127.3, 126.3 (4 x CH_{arom}), 126.2 (CH_{trz}), 126.0, 115.8 (2 x CH_{arom}), 41.9 (NCH₃). Anal. Calcd. For C₁₄H₁₂F₃N₅O₃S (387.34 g mol⁻¹): C, 43.41; H, 3.12; N, 18.08 %. Found: C, 43.69; H, 3.04; N, 17.72 %.

Synthesis of L2. A suspension of 1-(2-pyridyl)-4-(2-phenyl)triazole (649 mg, 2.92 mmol) and MeOTf (384 μL, 3.50 mmol) in dry CH₂Cl₂ (5 mL) was stirred at 0 °C for 30 min and

subsequently at r.t for 1 h. The solvent was evaporated under reduced pressure. The residue was precipitated and washed with Et₂O to obtain **L2** as a white solid. (1.082 g, 96%). ¹H NMR (CDCl₃, 400 MHz, 298 K): δ 9.04 (s, 1H, H_{trz}), 8.60 (d, *J*_{HH} = 4.0 Hz, 1H, H_{py}), 8.23 (d, *J*_{HH} = 8.1 Hz, 1H, H_{py}), 8.09 (td, *J*_{HH} = 8.1, 1.7 Hz, 1H, H_{py}), 7.74 (dd, *J*_{HH} = 7.8, 1.5 Hz, 2H, H_{ph}), 7.68–7.56 (m, 4H, H_{py} + H_{ph}), 4.43 (s, 3H, NCH₃). ¹³C NMR (CDCl₃, 100.6 MHz, 298 K): δ 149.3 (CH), 146.7 (C_{py}), 144.5 (C_{trz}), 140.6 (CH_{py}), 132.3 (CH_{ph}), 129.9 (CH_{ph}), 129.8 (CH_{ph}), 127.2 (CH_{py}), 124.5 (CH_{trz}), 121.8 (C_{ph}), 115.7 (CH_{py}), 39.5 (NCH₃). Anal. Calcd. For C₁₅H₁₃F₃N₄O₃S (386.35 g mol⁻¹): C, 46.63; H, 3.39; N, 14.75 %. Found: C, 46.23; H, 3.10; N, 14.43 %.

Synthesis of 1. A mixture of **L1** (150 mg, 0.39 mmol), Ag₂O (112 mg, 0.48 mmol) and [IrCl₂Cp*]₂ (193 mg, 0.24 mmol) in dry CH₂Cl₂ (15 mL) was stirred at room temperature for 48 h. After filtration through Celite and solvent evaporation, the yellowish residue was purified by gradient flash chromatography (SiO₂, CH₂Cl₂/MeOH 40:1 to 20:1). The product was isolated as a yellow solid (280 mg, 96%). IR (cm⁻¹): ν (py) 2915 (w). ¹H NMR (CDCl₃, 400 MHz, 298 K): δ = 8.87 (ddd, *J*_{HH} = 4.8, 1.7, 0.9 Hz, 1H, H_{py}), 8.73 (dd, *J*_{HH} = 5.7, 0.6 Hz, 1H, H_{py}), 8.38 (dd, *J*_{HH} = 8.2, 0.6 Hz, 1H, H_{py}), 8.30 (ddd, *J*_{HH} = 8.2, 7.4, 1.4 Hz, 1H, H_{py}), 8.06 (d, *J*_{HH} = 7.7 Hz, 1H, H_{py}), 7.93 (td, *J*_{HH} = 7.7, 1.7 Hz, 1H, H_{py}), 7.80 (ddd, *J*_{HH} = 7.4, 5.7, 1.4 Hz, 1H, H_{py}), 7.54 (ddd, *J*_{HH} = 7.7, 4.8, 1.2 Hz, 1H, H_{py}), 4.49 (s, 3H, NCH₃), 1.55 (s, 15H, Cp-CH₃). ¹³C NMR (CD₂Cl₂, 100.6 MHz, 298 K): δ = 153.3 (s, Ir-C_{trz}), 151.7, 150.5 (2 x CH_{py}), 150.1 (C_{py}), 146.1 (C_{py}), 143.9 (C_{trz}), 142.7, 137.7, 128.0, 127.3, 125.4, 115.1 (6 x CH_{py}), 91.9 (C_{Cp*}), 39.8 (NCH₃), 9.23 (Cp-CH₃). Anal. Calcd. For C₂₄H₂₆ClF₃IrN₅O₃S (749.22 g mol⁻¹): C, 38.47; H, 3.50; N, 9.35 %. Found: C, 38.30; H, 3.30; N, 9.07 %.

Synthesis of 2. A mixture of **L2** (200 mg, 0.52 mmol), Ag₂O (150 mg, 0.65 mmol) and [IrCl₂Cp*]₂ (258 mg, 0.32 mmol) in dry CH₂Cl₂ (15 mL) was stirred at room temperature for 36 h. After filtration through Celite and solvent evaporation, the yellowish residue was purified by flash chromatography (SiO₂, CH₂Cl₂/MeOH 20:1). The product was isolated as a yellow solid (420 mg, 95%). IR (cm⁻¹): ν (py) 2915 (w). ¹H NMR (CDCl₃, 500 MHz, 298 K): δ = 8.68 (d, *J*_{HH} = 5.6 Hz, 1H, H_{py}), 8.30 (d, *J*_{HH} = 8.3 Hz, 1H, H_{py}), 8.18 (ddd, *J*_{HH} = 8.3, 7.3, 1.2, 2H, H_{py}), 7.91–7.79 (m, 2H, H_{ph}), 7.63 (ddd, *J*_{HH} = 7.3, 5.6, 1.2 Hz, 1H, H_{py}), 7.61–7.54 (m, 3H, H_{ph}), 4.29 (s, 3H, NCH₃), 1.52 (s, 15H, Cp-CH₃). ¹³C NMR (CDCl₃, 125.8 MHz, 298 K): δ = 151.9 (Ir-C_{trz}), 151.0 (C_{py}), 150.9 (CH_{py}), 146.1 (C_{trz}), 141.9 (CH_{py}), 131.5 (CH_{ph}), 131.0 (CH_{ph}), 129.4 (CH_{ph}), 126.8 (CH_{py}), 126.1 (C_{ph}), 114.9 (CH_{py}), 91.7 (C_{Cp*}), 38.6 (NCH₃), 9.1

(Cp-CH₃). Anal. Calcd. For C₂₅H₂₇ClF₃IrN₄O₃S (748.24 g mol⁻¹): C, 40.13; H, 3.64; N, 7.49 %. Found: C, 39.87; H, 3.53; N, 7.21 %.

Synthesis of 3. A mixture of **1** (100 mg, 0.134 mmol), AgOTf (38 mg, 0.15 mmol) and aniline (13.4 μL, 0.146 mmol) in dry CH₂Cl₂ (5 mL) was stirred at room temperature for 18 h, protected from light. After filtration through Celite, the brown solution was concentrated to about 0.5 mL. Addition of Et₂O (4 mL) induced precipitation of the product as a yellow solid, which was washed with Et₂O (3 x 4 mL) and subsequently dried in vacuo (light yellow solid, 112 mg, 87%). IR (cm⁻¹): ν (NH) 3240, 3203, 3125, 3079 (w). ¹H NMR (acetone-*d*₆, 500 MHz, 298 K): δ = 9.15 (d, *J*_{HH} = 5.6 Hz, 1H, H_{py}), 9.06 (ddd, *J*_{HH} = 4.8, 1.7, 0.9 Hz, 1H, H_{py}), 8.47 (ddd, *J*_{HH} = 8.2, 7.5, 1.2 Hz, 1H, H_{py}), 8.36 (d, *J*_{HH} = 7.7 Hz, 1H, H_{py}), 8.30 (td, *J*_{HH} = 7.7, 1.7 Hz, 1H, H_{py}), 8.14 (dd, *J*_{HH} = 8.2, 0.8 Hz, 1H, H_{py}), 7.98 (ddd, *J*_{HH} = 7.5, 5.6, 0.8 Hz, 1H, H_{py}), 7.83 (ddd, *J*_{HH} = 7.7, 4.8, 1.2 Hz, 1H, H_{py}), 7.48–7.34 (m, 2H, NH₂), 6.92 (t, *J*_{HH} = 7.4 Hz, 1H, H_{ph}), 6.87 (t, *J*_{HH} = 7.4 Hz, 2H, H_{ph}), 6.59 (d, *J*_{HH} = 7.4 Hz, 2H, H_{ph}), 4.53 (s, 3H, NCH₃), 1.68 (s, 15H, Cp-CH₃). ¹³C NMR (acetone-*d*₆, 125.8 MHz, 298 K): δ = 153.2 (CH_{py}), 153.2 (Ir-C_{trz}), 152.0 (CH_{py}), 151.0 (C_{py}), 146.2 (C_{py}), 145.4 (C_{trz}), 144.4 (CH_{py}), 140.4 (C_{ph}), 139.4 (CH_{py}), 129.5 (CH_{ph}), 129.4, 128.4, 126.8 (3 x CH_{py}), 125.9 (CH_{ph}), 121.5 (CH_{ph}), 115.6 (CH_{py}), 93.5 (C_{Cp*}), 40.2 (NCH₃), 9.1 (Cp-CH₃). Anal. Calcd. For C₃₁H₃₃F₆IrN₆O₆S₂ (955.96 g mol⁻¹): C, 38.95; H, 3.48; N, 8.79 %. Found: C, 38.78; H, 3.38; N, 8.41 %.

Synthesis of 3'. A solution of NaBPh₄ (90 mg, 0.26 mmol) in 0.5 mL of MeOH was added to a solution of **3** (50 mg, 0.052 mmol) in 0.5 mL of MeOH. A pale yellow solid precipitated. The supernatant was removed and the solid was washed with MeOH (4 x 1 mL) and Et₂O (3 x 5 mL) and subsequently dried in vacuo (pale yellow solid, 32 mg, 47%). ¹H NMR (acetone-*d*₆, 400 MHz, 298 K): δ = 9.18 (dd, *J*_{HH} = 5.7, 0.7 Hz, 1H, H_{py}), 9.04 (ddd, *J*_{HH} = 4.8, 1.5, 1.1 Hz, 1H, H_{py}), 8.31 (ddd, *J*_{HH} = 8.2, 7.5, 1.5 Hz, 1H, H_{py}), 8.27–8.17 (m, 2H, H_{py}), 8.06 (d, *J*_{HH} = 8.2 Hz, 1H, H_{py}), 7.89 (ddd, *J*_{HH} = 7.5, 5.7, 1.5 Hz, 1H, H_{py}), 7.79 (ddd, *J*_{HH} = 7.1, 4.8, 1.6 Hz, 1H, H_{py}), 7.48–7.39 (br s, 2H, NH₂), 7.38–7.29 (m, 16H, H_{BPh4}), 6.98–6.84 (m, 16H, H_{BPh4} + 3H, H_{aniline}), 6.77 (t, *J*_{HH} = 7.2 Hz, 8H, H_{BPh4}), 6.57 (d, *J*_{HH} = 7.9 Hz, 2H, H_{aniline}), 4.43 (s, 3H, NCH₃), 1.65 (s, 15H, Cp-CH₃). ¹³C NMR (acetone-*d*₆, 100.6 MHz, 298 K): δ = 165.7 (q, *J*_{BC} = 49.5 Hz, C_{BPh4}), 153.5 (Ir-C_{trz}), 153.1, 152.1 (2 x CH_{py}), 150.9 (C_{py}), 146.0 (C_{py}), 145.7 (C_{trz}), 144.7 (CH_{py}), 140.0 (C_{aniline}), 139.2 (CH_{py}), 137.0 (q, *J*_{BC} = 1.7 Hz, CH_{BPh4}), 129.8 (CH_{aniline}), 129.6 (CH_{py}), 127.6 (CH_{aniline}), 127.0, 126.4 (2 x CH_{py}), 126.0 (q, *J*_{BC} = 2.7 Hz, CH_{BPh4}), 122.3 (CH_{BPh4}), 121.2 (CH_{aniline}), 115.7 (CH_{py}), 93.6 (C_{Cp*}), 40.1 (NCH₃), 9.1 (Cp-CH₃). Anal. Calcd.

For $C_{77}H_{73}B_2IrN_6$ (1296.28 g mol⁻¹): C, 71.34; H, 5.68; N, 6.48 %. Found: C, 71.14; H, 5.52; N, 6.18 %.

Synthesis of 4. A mixture of **1** (150 mg, 0.20 mmol), AgOTf (56 mg, 0.22 mmol) and benzylamine (24 μ l, 0.22 mmol) in dry CH_2Cl_2 (15 mL) was stirred at room temperature for 18 h. After filtration through Celite, the yellow solution was concentrated to about 1 mL. Addition of Et_2O (50 mL) induced precipitation of the product as a pale yellow solid, which was washed with Et_2O (3 x 20 mL) and subsequently dried in vacuo (pale yellow solid, 167 mg, 87%). IR (cm⁻¹): ν (NH) 3236, 3149 (w). ¹H NMR (acetone-*d*₆, 500 MHz, 298 K): δ = 9.30 (ddd, J_{HH} = 5.7, 1.4, 0.7 Hz, 1H, H_{py}), 9.01 (ddd, J_{HH} = 4.8, 1.7, 1.0 Hz, 1H, H_{py}), 8.59 (ddd, J_{HH} = 8.3, 7.3, 1.4 Hz, 1H, H_{py}), 8.53 (ddd, J_{HH} = 8.3, 1.3, 0.7 Hz, 1H, H_{py}), 8.21 (td, J_{HH} = 7.7, 1.7 Hz, 1H, H_{py}), 8.15 (dd, J_{HH} = 7.7, 1.2 Hz, 1H, H_{py}), 8.01 (ddd, J_{HH} = 7.3, 5.7, 1.3 Hz, 1H, H_{py}), 7.77 (ddd, J_{HH} = 7.7, 4.8, 1.2 Hz, 1H, H_{py}), 7.36–6.98 (m, 5H, H_{Ph}), 5.59–5.49 (m, 1H, NH₂), 5.33–5.23 (m, 1H, NH₂), 4.53 (s, 3H, NCH₃), 4.08–4.00 (m, 1H, CH₂), 3.81–3.73 (m, 1H, CH₂), 1.68 (s, 15H, Cp–CH₃). ¹³C NMR (acetone-*d*₆, 125.8 MHz, 298 K): δ = 153.6 (CH_{py}), 152.1 (C_{py}), 151.7 (CH_{py}), 150.7 (Ir–C_{trz}), 146.5 (C_{trz}), 146.3 (C_{py}), 144.7, 139.2 (2 x CH_{py}), 139.0 (C_{Ph}), 129.5, 129.4 (2 x CH_{Ph}), 129.1 (CH_{py}), 128.9 (CH_{Ph}), 128.1, 126.6, 116.2 (3 x CH_{py}), 93.2 (C_{Cp*}), 53.8 (CH₂), 40.1 (NCH₃), 8.98 (Cp–CH₃). Anal. Calcd. For $C_{32}H_{35}F_6IrN_6O_6S_2$ (969.99 g mol⁻¹): C, 39.62; H, 3.64; N, 8.66 %. Found: C, 39.78; H, 3.49; N, 8.32 %.

Synthesis of 4'. A solution of NaBPh₄ (264 mg, 0.773 mmol) in 1 mL of MeOH was added to a solution of **4** (150 mg, 0.154 mmol) in MeOH (0.6 mL). A pale yellow solid precipitated. The supernatant was removed and the solid was washed with copious amounts of MeOH (10 mL in total) and Et_2O (3 x 10 mL) and subsequently dried in vacuo. (pale yellow solid, 143 mg, 71%). ¹H NMR (acetone-*d*₆, 500 MHz, 298 K): δ = 9.24 (d, J_{HH} = 5.7 Hz, 1H, H_{py}), 9.01 (ddd, J_{HH} = 4.8, 1.7, 0.9 Hz, 1H, H_{py}), 8.51 (dd, J_{HH} = 8.1, 1.4 Hz, 1H, H_{py}), 8.48 (ddd, J_{HH} = 8.1, 7.3, 1.3 Hz, 1H, H_{py}), 8.19 (td, J_{HH} = 7.7, 1.7 Hz, 1H, H_{py}), 8.13 (d, J_{HH} = 7.7 Hz, 1H, H_{py}), 7.98 (ddd, J_{HH} = 7.3, 5.7, 1.4 Hz, 1H, H_{py}), 7.77 (ddd, J_{HH} = 7.7, 4.8, 1.1 Hz, 1H, H_{py}), 7.37–7.20 (m, 16H, H_{BPh4}), 7.28–7.24 (m, 3H, H_{Ph}), 7.12–7.09 (m, 2H, H_{Ph}), 6.91 (t, J_{HH} = 7.3 Hz, 16H, H_{BPh4}), 6.77 (t, J_{HH} = 7.3 Hz, 8H, H_{BPh4}), 5.52 (t, J_{HH} = 11.0 Hz, 1H, NH₂), 5.29 (t, J_{HH} = 11.0 Hz, 1H, NH₂), 4.49 (s, 3H, NCH₃), 4.16 (ddd, J_{HH} = 14.8, 11.0, 3.3 Hz, 1H, CH₂), 3.85 (ddd, J_{HH} = 14.8, 11.0, 3.5 Hz, 1H, CH₂), 1.67 (s, 15H, Cp–CH₃). ¹³C NMR (acetone-*d*₆, 125.8 MHz, 298 K): δ = 164.9 (q, J_{BC} = 49.5 Hz, 8 x C_{BPh4}), 153.4, 152.1, 152.0 (3 x CH_{py}), 151.4 (Ir–C_{trz}), 146.8 (C_{trz}), 146.0, 145.1, 139.2 (3 x CH_{py}), 139.1 (C_{Ph}), 137.0 (q, J_{BC} = 1.3 Hz, CH_{BPh4}), 129.7 (CH_{Ph}), 129.4 (CH_{py}), 129.3 (s, CH_{Ph}), 129.1 (CH_{Ph}), 127.6, 126.9 (2 x CH_{py}), 126.0 (q, J_{BC} = 2.8 Hz, CH_{BPh4}),

122.2 (CH_{BPh4}), 116.2 (CH_{py}), 93.3 (C_{Cp*}), 53.9 (CH₂), 40.1 (NCH₃), 9.0 (Cp-CH₃). Anal. Calcd. For C₇₈H₇₅B₂IrN₆ (1310.31 g mol⁻¹): C, 71.50; H, 5.77; N, 6.41 %. Found: C, 71.32; H, 5.63; N, 6.26 %.

Synthesis of 5. A mixture of **2** (100 mg, 0.134 mmol), AgOTf (38 mg, 0.15 mmol) and aniline (13.4 μ l, 0.146 mmol) in dry CH₂Cl₂ (5 mL) was stirred at room temperature for 18 h, protected from light. After filtration through Celite, the brown solution was concentrated to about 0.5 mL. Addition of die Et₂O (4 mL) induced precipitation of the product as an ivory solid, which was washed with Et₂O (3 x 20 mL) and subsequently dried in vacuo (ivory solid, 94 mg, 74%). IR (cm⁻¹): ν (NH) 3227, 3202, 3132 (w). ¹H NMR (acetone-*d*₆, 400 MHz, 298 K): δ = 9.00 (dd, J_{HH} = 5.7, 1.0 Hz, 1H, H_{py}), 8.44 (ddd, J_{HH} = 8.2, 7.5, 1.0 Hz, 1H, H_{py}), 8.11 (d, J_{HH} = 8.2 Hz, 1H, H_{py}), 8.08–8.00 (m, 2H, H_{Ph}), 7.94 (ddd, J_{HH} = 7.5, 5.7, 1.2 Hz, 1H, H_{py}), 7.85–7.76 (m, 3H, H_{Ph}), 7.48–7.33 (m, 2H, NH₂), 6.96 (t, J_{HH} = 7.3 Hz, 1H, H_{aniline}), 6.90 (t, J_{HH} = 7.3 Hz, 2H, H_{aniline}), 6.49 (d, J_{HH} = 8.0 Hz, 2H, H_{aniline}), 4.38 (s, 3H, NCH₃), 1.66 (s, 15H, Cp-CH₃). ¹³C NMR (acetone-*d*₆, 100.6 MHz, 298 K): δ = 152.9 (CH_{py}), 151.3 (Ir-C_{trz}), 151.1 (C_{py}), 147.1 (C_{trz}), 144.4 (CH_{py}), 140.4 (C_{aniline}), 132.3 (CH_{Ph}), 132.2 (CH_{Ph}), 130.5 (CH_{Ph}), 129.7 (CH_{aniline}), 129.4 (CH_{py}), 126.3 (C_{Ph}), 125.9 (CH_{aniline}), 121.4 (CH_{aniline}), 115.5 (CH_{py}), 93.4 (C_{Cp*}), 39.4 (NCH₃), 9.9 (Cp-CH₃). Anal. Calcd. For C₃₂H₃₄F₆IrN₅O₆S₂ (954.98 g mol⁻¹)·0.1 CH₂Cl₂: C, 40.02; H, 3.58; N, 7.27 %. Found: C, 39.69; H, 3.96; N, 7.08 %.

Synthesis of 6. A mixture of **2** (100 mg, 0.134 mmol), AgOTf (38 mg, 0.15 mmol) and benzylamine (16 μ l, 0.15 mmol) in dry CH₂Cl₂ (10 mL) was stirred at room temperature for 18 h. After filtration through Celite, the yellow solution was concentrated to about 1 mL. Addition of Et₂O (50 mL) induced precipitation of the product as a pale yellow solid, which was washed with Et₂O (3 x 20 mL) and subsequently dried in vacuo (pale yellow solid, 97 mg, 75%). IR (cm⁻¹): ν (NH) 3239, 3165 (w). ¹H NMR (acetone-*d*₆, 400 MHz, 298 K): δ = 9.29 (d, J_{HH} = 5.6 Hz, 1H, H_{py}), 8.60 (ddd, J_{HH} = 8.0, 7.3, 1.3 Hz, 1H, H_{py}), 8.54 (dd, J_{HH} = 8.0, 1.1 Hz, 1H, H_{py}), 8.02 (ddd, J_{HH} = 7.3, 5.6, 1.1 Hz, 1H, H_{py}), 7.91–7.84 (m, 2H, H_{Ph}), 7.75–7.69 (m, 3H, H_{Ph}), 7.26–7.19 (m, 5H, H_{BnNH2}), 5.48–5.32 (m, 2H, NH₂), 4.36 (s, 3H, NCH₃), 3.86–3.63 (m, CH, CH₂), 1.67 (s, 15H, Cp-CH₃). ¹³C NMR (acetone-*d*₆, 100.6 MHz, 298 K): δ = 153.4 (CH_{py}), 152.3 (C_{py}), 149.3 (Ir-C_{trz}), 147.8 (C_{trz}), 144.7 (CH_{py}), 138.7 (C_{BnNH2}), 132.3 (CH_{Ph}), 132.0 (CH_{Ph}), 130.4 (CH_{Ph}), 129.7, 129.5 (2 x CH_{BnNH2}), 129.1 (CH_{py}), 129.0 (CH_{BnNH2}), 126.5 (C_{Ph}), 116.2 (CH_{py}), 93.1 (C_{Cp*}), 53.9 (CH₂), 39.4 (NCH₃), 8.9 (Cp-CH₃). Anal. Calcd. For C₃₃H₃₆F₆IrN₅O₆S₂ (969.00 g mol⁻¹)·0.2 Et₂O: C, 41.26; H, 3.89; N, 7.12 %. Found: C, 41.09; H, 4.26; N, 7.18 %.

Synthesis of 7. A mixture of **3** (20 mg, 0.021 mmol), AgOTf (6 mg, 0.023 mmol) and aniline (31 μ l, 0.31 μ l) in dry CH₂Cl₂ (1 mL) was stirred at room temperature for 18 h. Addition of Et₂O (4 mL) induced precipitation of the product as a yellow solid, which was washed with Et₂O (3 x 4 mL) and subsequently dried *in vacuo* (ivory solid, 21 mg, 81%). Recrystallization from CH₂Cl₂/Et₂O was performed in a flask wrapped with aluminium foil to protect the complex from light. IR (cm⁻¹): ν (NH) 3235, 3201, 3124, 3077 (w). ¹H NMR (acetone-*d*₆, 400 MHz, 298 K): δ = 9.09 (d, J_{HH} = 5.0 Hz, 2H, H_{py}), 8.44 (m, 2H, H_{py}), 8.35 (td, J_{HH} = 7.5, 1.6 Hz, 1H, H_{py}), 8.10 (d, J_{HH} = 8.1 Hz, 1H, H_{py}), 7.95 (ddd, J_{HH} = 7.5, 5.0, 1.1 Hz, 1H, H_{py}), 7.89 (ddd, J_{HH} = 7.5, 5.0, 1.2 Hz, 1H, H_{py}), 7.45–7.29 (m, 2H, NH₂), 6.93 (t, J_{HH} = 7.2 Hz, 1H, H_{aniline}), 6.87 (t, J_{HH} = 7.4 Hz, 2H, H_{aniline}), 6.56 (d, J_{HH} = 7.8 Hz, 2H, H_{aniline}), 4.51 (s, 3H, NCH₃), 1.68 (s, 15H, Cp–CH₃). ¹³C NMR (acetone-*d*₆, 100.6 MHz, 298 K): δ = 153.1 (CH_{py}), 153.1 (Ir–C_{trz}), 152.7 (CH_{py}), 151.0 (C_{py}), 146.2 (C_{py}), 145.3 (C_{trz}), 144.4 (CH_{py}), 140.4 (C_{aniline}), 140.1 (CH_{py}), 129.6 (2 x CH_{aniline}), 129.4 (CH_{py}), 129.1 (CH_{py}), 127.2 (CH_{py}), 125.9 (CH_{aniline}), 121.5 (CH_{aniline}), 115.6 (CH_{py}), 93.6 (C_{Cp*}), 40.2 (NCH₃), 9.1 (Cp–CH₃). Anal. Calcd. For C₃₂H₃₅AgF₉IrN₆O₁₀S₃ (1230.92 g mol⁻¹): C, 31.22; H, 2.87; N, 6.83. Found: C, 31.49; H, 2.97; N, 6.94 %. HRMS (ESI⁺, 27V): m/z : 807.1909; calculated for [M–Ag –H₂O–(CF₃SO₃)₂]⁺ 807.1911.

Synthesis of 8. A mixture of **4** (20 mg, 0.021 mmol), AgOTf (5.9 mg, 0.023 mmol) in dry CH₂Cl₂ (1 mL) was stirred at room temperature for 18 h protected against the light. After solvent evaporation, the residue was dissolved in acetone (2 mL) and filtered through Celite. The yellow solution was concentrated to about 0.5 mL. Addition of Et₂O (2 mL) induced precipitation of a solid, which was washed with Et₂O (3 x 2 mL) and subsequently dried *in vacuo* (ivory solid, 14 mg, 54%). IR (cm⁻¹): ν (NH) 3233, 3150 (w). ¹H NMR (acetone-*d*₆, 400 MHz, 298 K): δ = 9.27 (d, J_{HH} = 5.7 Hz, 1H, H_{py}), 9.08 (ddd, J_{HH} = 5.0, 1.6, 0.9 Hz, 1H, H_{py}), 8.63–8.56 (m, 1H, H_{py}), 8.52 (dd, J_{HH} = 7.8, 1.2 Hz, 1H, H_{py}), 8.30 (td, J_{HH} = 7.8, 1.6 Hz, 1H, H_{py}), 8.17 (td, J_{HH} = 7.8, 0.9 Hz, 1H, H_{py}), 8.01 (ddd, J_{HH} = 7.8, 5.7, 1.4 Hz, 1H, H_{py}), 7.87 (ddd, J_{HH} = 7.8, 5.0, 1.2 Hz, 1H, H_{py}), 7.25–7.19 (m, 5H, H_{BnNH2}), 5.48–5.25 (m, 2H, NH₂), 4.49 (s, 3H, NCH₃), 4.02–3.85, 3.83–3.58 (2 x m, 1H, CH₂), 1.68 (s, 15H, Cp–CH₃). ¹³C NMR (acetone-*d*₆, 100.6 MHz, 298 K): δ = 153.4, 152.9 (2 x CH_{py}), 152.1 (C_{py}), 150.7 (Ir–C_{trz}), 146.4 (C_{trz}), 146.1 (C_{py}), 144.7, 140.4 (2 x CH_{py}), 138.7 (C_{BnNH2}), 129.6 (CH_{BnNH2}), 129.4 (CH_{py}), 129.3, 128.9 (2 x CH_{BnNH2}), 128.8, 127.2, 116.6 (3 x CH_{py}), 93.3 (C_{Cp*}), 53.8 (CH₂), 40.1 (NCH₃), 9.05 (Cp–CH₃). Anal. Calcd. for C₃₃H₃₇AgF₉IrN₆O₁₀S₃ (1244.95 g mol⁻¹): C, 31.84; H, 3.00; N, 6.75 %. Found: C, 31.68; H, 3.03; N, 6.53 %.

General Procedure for oxidative coupling of amines.

A mixture of amine (0.2 mmol) and the iridium complex (0.01 mmol) in 1,2-dichlorobenzene (2 mL) was heated at 150 °C in a closed vial. The reaction mixture was analyzed by ¹H NMR spectroscopy using Hexamethylbenzene (0.033 mmol) as internal standard. The signals due to reagents and products were identified according to commercially available samples (benzylamine, 4-methoxybenzylamine, 4-methylbenzylamine, 4-chlorobenzylamine, 3-chlorobenzylamine, α -methylbenzylamine, N-benzylidenbenzylamine, dibenzylamine, tribenzylamine) or previously reported spectroscopic data (N-(4-chlorobenzylidene)-4-chlorobenzylamine, N-(3-chlorobenzylidene)-3-chlorobenzylamine, *p*-methyl-N-(*p*-methylbenzylidene)benzylamine, *p*-methoxy-N-(*p*-methoxybenzylidene)benzylamine,^[9f] N-(α -methylbenzylidene)- α -methylbenzylamine,^[45a] bis-(4-methoxybenzyl)amine, bis-(4-chlorobenzyl)amine,^[45b] bis(3-chlorobenzyl)amine,^[45c] bis(4-methylbenzyl)amine,^[45d] bis(1-phenylethyl)amine,^[45e] tris(4-methoxybenzyl)amine, tris(4-methylbenzyl)amine, tris(4-chlorobenzyl)amine,^[45f] and tris(3-chlorobenzyl)amine.^[45g]

Crystallographic analyses.

Crystal data for complexes **1**, **2**, **4'** and **7** were collected by using an Agilent Technologies (now Rigaku) SuperNova A diffractometer fitted with an Atlas detector using Mo-K α radiation (0.71073 Å). A complete dataset was collected, assuming that the Friedel pairs are not equivalent. An analytical numeric absorption correction was performed.^[46] Crystal data for complex **3** was collected on an Oxford Diffraction SuperNova area-detector diffractometer^[47] using mirror optics monochromated Mo K α radiation ($\lambda = 0.71073$ Å) and Al filtered.^[48] The unit cell constants and an orientation matrix for data collection were obtained from a least-squares refinement of the setting angles of reflections in the range $1.8^\circ < \theta < 27.9^\circ$. A total of 1428 frames were collected using ω scans, with 20+20 seconds exposure time, a rotation angle of 1.0° per frame, a crystal-detector distance of 65.0 mm, at T = 123(2) K. Data reduction was performed using the *CrysAlisPro*^[47] program. The intensities were corrected for Lorentz and polarization effects, and a numerical absorption correction based on gaussian integration over a multifaceted crystal model was applied. The structure of **1**, **2**, **4'** and **7** were solved by direct methods using SHELXS-97 and refined by full-matrix least-squares fitting on F² for all data using SHELXL-97.^[49] Hydrogen atoms were added at calculated positions and refined by using a riding model. Their isotropic temperature factors were fixed to 1.2 times (1.5 times for methyl

groups) the equivalent isotropic displacement parameters of the carbon atom the H-atom is attached to. Anisotropic thermal displacement parameters were used for all nonhydrogen atoms. The structure of **3'** was solved by direct methods using SHELXT,^[50] which revealed the positions of all not disordered non-hydrogen atoms of the title compound. The non-hydrogen atoms were refined anisotropically. All H-atoms were placed in geometrically calculated positions and refined using a riding model where each H-atom was assigned a fixed isotropic displacement parameter with a value equal to 1.2Ueq of its parent atom (1.5Ueq for the methyl groups). Refinement of the structure **3'** was carried out on F^2 using full-matrix least-squares procedures, which minimized the function $\Sigma w(F_o^2 - F_c^2)^2$. The weighting scheme was based on counting statistics and included a factor to downweight the intense reflections. All calculations were performed using the SHELXL-2014/7^[51] program. The crystal contains one metal complex with two co-crystallized tetraphenylborate anions and one dichloromethane molecule in the asymmetric unit. There are more co-crystallized heavily disordered dichloromethane and ether molecules present in the crystal which however could not modelled successfully. The remaining electron density in the solvent accessible voids was therefore accounted for with the PLATON^[52] SQUEEZE procedure. Crystallographic details are compiled in Tables S1–S5. CCDC No 1526895 (**1**), 1526897 (**2**), 1526899 (**3'**), 1526898 (**4'**), and 1526896 (**7**) contain the supplementary crystallographic data for this paper. These data can be obtained free of charge from the Cambridge Crystallographic Data Centre via www.ccdc.cam.ac.uk/data_request/cif.

Supporting information available: Crystallographic details, and structure data in cif format; comparative NMR and IR spectra.

Acknowledgment

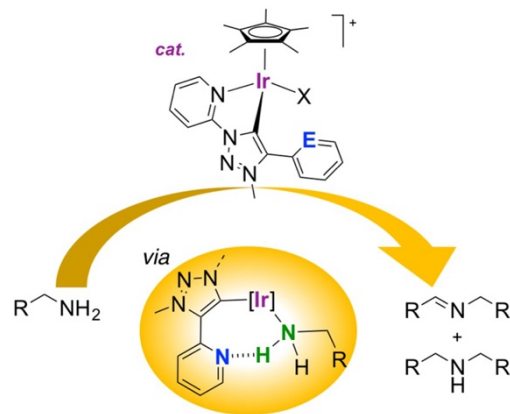
We thank Dr. J. Hauser (Univ Bern) for solving the crystal structure of complex **3'**. The authors gratefully acknowledge financial support from the European Commission (ERC CoG 615653), the Marie SkłodowskaCurie Action for a fellowship to M.V. (grant 660929) as well as the Swiss National Science Foundation (200021–162868 and 206021–128724). A.P. thanks MEC for a FPU fellowship and COST CM1205 CARISMA for a STSM visiting fellowship.

Keywords

Iridium --- triazolylidene ---- ligand metal cooperativity --- hydrogen bonding --- amine dehydrogenation

Entry for Table of Contents:

A pending pyridyl group in the C,N-bidentate chelating carbene-pyridyl complex **1** facilitates amine coordination to the iridium center and enhances catalytic activity of the metal center in amine dehydrogenation. Stoichiometric experiments provide evidence for hydrogen bonding of the amine substrate with the pending pyridyl unit.



References

- [1] a) S.-I. Murahashi, *Angew. Chem., Int. Ed.* **1995**, *34*, 2443–2465; b) S. Yao, S. Saaby, R. G. Hazell, K. A. Jørgensen, *Chem. Eur. J.* **2000**, *6*, 2435–2448; c) Z.-Y. Liu, Y.-M. Wang, Z.-R. Li, J.-D. Jiang, D. W. Boykin, *Bioorg. Med. Chem. Lett.* **2009**, *19*, 5661–5664; d) *The Chemistry of Anilines, Vol. 1* (Ed.: Z. Rappoport), Wiley- Interscience, New York, **2007**; e) J. F. Hartwig, *Handbook of Organopalladium Chemistry for Organic Synthesis, Vol. 1* (Eds.: E.-I. Negishi, A. Meijere), Wiley-Interscience, New York, **2002**, p. 1051.
- [2] a) H. Sun, F.-Z. Su, J. Ni, Y. Cao, H.-Y. He, K.-N. Fan, *Angew. Chem. Int. Ed.* **2009**, *48*, 4390–4393; b) B. Gnanaprakasam, J. Zhang, D. Milstein, *Angew. Chem., Int. Ed.* **2010**, *49*, 1468–1471; c) S. Kegnæs, J. Mielby, U. V. Mentzel, C. H. Christensen, A. Riisager, *Green Chem.* **2010**, *12*, 1437–1441; d) E. Sindhuja, R. Ramesh, *Tetrahedron Lett.* **2014**, *55*, 5504–5507.
- [3] For alternative pathways for amine coupling with alcohols to produce amides, see: a) Milstein: C. Gunanathan, Y. Ben-David, D. Milstein, *Science* **2007**, *317*, 790–792; b) L. U. Nordstrøm, H. Vogt, R. Madsen, *J. Am. Chem. Soc.*, **2008**, *130*, 17672–17673; c) T. Zweifel, J.-V. Naubron, H. Grützmacher, *Angew. Chem. Int. Ed.* **2009**, *48*, 559–563; c) D. Srimani, E. Balaraman, P. Hu, Y. Ben-David, D. Milstein *Adv. Synth. Catal.* **2013**, *355*, 2525–2530.
- [4] For secondary amine dehydrogenation see: a) H. Huang, J. Huang, Y.-M. Liu, H.-Y. He, Y. Cao, K.-N. Fan, *Green Chem.* **2012**, *14*, 930–934; b) D. Pinggen, M. Lutz, D. Vogt, *Organometallics* **2014**, *33*, 1623–1629; c) D. Pinggen, Ç. Altıntaş, M. R. Schaller, D. Vogt, *Dalton Trans.* **2016**, *45*, 11765–11771.
- [5] For homogeneous dehydrogenation and hydrogenation of tetrahydroquinolines and quinolines, see: a) R. Yamaguchi, C. Ikeda, T. Takahashi, K.-I. Fujita, *J. Am. Chem. Soc.* **2009**, *131*, 8410–8412; b) Z. Wang, I. Tonks, J. Belli, C.M. Jensen, *J. Organomet. Chem.* **2009**, *694*, 2854–2857; c) H. Li, J. Jiang, G. Lu, F. Huang, Z.-X. Wang, *Organometallics* **2011**, *30*, 3131–3141; d) G. E. Dobereiner, A. Nova, N. D. Schley, N. Hazari, S. J. Miller, O. Eisenstein, R. H. Crabtree, *J. Am. Chem. Soc.* **2011**, *133*, 7547–7562; e) J. Wu, D. Talwar, S. Johnston, M. Yan, J. Xiao, *Angew. Chem., Int. Ed.* **2013**, *52*, 6983–6987; f) K.-I. Fujita, Y. Tanaka, M. Kobayashi, R. Yamaguchi, *J. Am. Chem. Soc.* **2014**, *136*, 4829–4832; g) S. Chakraborty, W. W. Brennessel, W. D. Jones, *J. Am. Chem. Soc.* **2014**, *136*, 8564–8567.
- [6] For examples of catalytic dehydrogenation of other N-heterocycles, see: a) Y. Tsuji, S. Kotachi, K. T. Huh, Y. Watanabe, *J. Org. Chem.* **1990**, *55*, 580–584; b) T. Hara, K. Mori, T. Mizugaki, K. Ebitani, K. Kaneda, *Tetrahedron Lett.* **2003**, *44*, 6207–6210; c) D. Dean, B. Davis, P. G. Jessop, *New J. Chem.* **2011**, *35*, 417–422.
- [7] For cyclic amine dehydrogenation see: G. E. Dobereiner, R. H. Crabtree, *Chem. Rev.* **2010**, *110*, 681–703.
- [8] g) A. Grirrane, A. Corma, H. Garcia, *J Catal.* **2009**, *264*, 138–144; b) H. Guo, M. Kemell, A. Al-Hunaiti, S. Rautiainen, M. Leskelä, T. Repo, *Catal. Commun.* **2011**, *12* 1260–1264; c) M. T. Schümperli, C. Hammond, I. Hermans, *ACS Catal.* **2012**, *2*, 1108–1117; d) C. Hammond, M. T. Schümperli, I. Hermans, *Chem. Eur. J.* **2013**, *19*, 13193–13198; e) S. Furukawa, A. Suga, T. Komatsu, *Chem. Commun.* **2014**, *50*, 3277–3280; f) W. Deng, J. Chen, J. Kang, Q. Zhang, Y. Wang, *Chem. Commun.* **2016**, *52*, 6805–6808; g) P. Sudarsanam, B. Mallesham, A. Rangaswamy, B. G. Rao, S. K. Bhargava, B. M. Reddy,

- J. Mol. Cat. A: Chemical*, **2016**, *412*, 47–55; h) A. Rangaswamy, P. Sudarsanam, B. G. Rao, B. M. Reddy, *Res Chem Intermed*, **2016**, *42* 4937–4950.
- [9] a) D. Hollmann, S. Bähn, A. Tillack, M. Beller, *Angew. Chem. Int. Ed.* **2007**, *46*, 8291–8294; b) A. Prades, R. Corberán, M. Poyatos, E. Peris, *Chem. Eur. J.* **2008**, *14*, 11474–11479; c) D. Hollmann, S. Bähn, A. Tillack, R. Parton, R. Altink, M. Beller, *Tetrahedron Lett.* **2008**, *49*, 5742–5745; d) D. Hollmann, S. Bähn, A. Tillack, M. Beller, *Chem. Commun.*, **2008**, 3199–3201; e) A. Prades, E. Peris, M. Albrecht, *Organometallics* **2011**, *30*, 1162–1167; f) S. Zhao, C. Liu, Y. Guo, J.-C. Xiao, Q.-Y. Chen, *J. Org. Chem.* **2014**, *79*, 8926–8931; g) D. Wang, K. Zhao, C. Xu, H. Miao, Y. Ding, *ACS Catal.* **2014**, *4*, 3910–3918; h) Q. Zou, C. Wang, J. Smith, D. Xue, J. Xiao, *Chem. Eur. J.* **2015**, *21*, 9656–9661; i) Y. Zhang, F. Lu, R. Huang, H. Zhang, J. Zhao, *Cata. Commun.* **2016**, *81*, 10–13.
- [10] J. F. Hartwig, *Organotransition Metal Chemistry: From Bonding to Catalysis*, University Science Books, Sausalito, CA, **2010**.
- [11] a) G. C. Welch, R. R. San Juan, J. D. Masuda, D. W. Stephan, *Science* **2006**, *314*, 1124–1126; b) P. P. Power *Nature* **2010**, *463*, 171–177; c) D. W. Stephan, G. Erker, *Angew. Chem. Int. Ed.* **2010**, *49*, 46–76.
- [12] a) R. Noyori, T. Ohkuma, *Angew. Chem. Int. Ed.* **2001**, *40*, 40–73; b) S. Kuwata, T. Ikariya, *Chem. Commun.* **2014**, *50*, 14290–14300; c) J. R. Khusnutdinova, D. Milstein, *Angew. Chem. Int. Ed.* **2015**, *54*, 12236–12273.
- [13] S. Sabater, H. Müller-Bunz, M. Albrecht, *Organometallics* **2016**, *35*, 2256–2266.
- [14] C. H. Leung, C. D. Incarvito, R. H. Crabtree, *Organometallics* **2006**, *25*, 6099–6107.
- [15] J. C. C. Chen, I. J. B. Lin, *Organometallics*, **2000**, *19*, 5113–5121.
- [16] a) R. Lalrempuia, N. D. McDaniel, H. Müller-Bunz, S. Bernhard, M. Albrecht, *Angew. Chem Int. Ed.* **2010**, *49*, 9765–9768; b) K. F. Donnelly, R. Lalrempuia, H. Müller-Bunz, M. Albrecht, *Organometallics* **2012**, *31*, 8414–8419; c) C. M. Álvarez, L. A. García-Escudero, R. García-Rodríguez, D. Miguel, *Chem. Commun.* **2012**, *48*, 7209–7211; d) M. Delgado-Rebollo, D. Canseco-Gonzalez, M. Hollering, H. Müller-Bunz, M. Albrecht, *Dalton Trans.* **2014**, *43*, 4462–4473; e) S. Hohloch, L. Hettmanczyk, B. Sarkar, *Eur. J. Inorg. Chem.* **2014**, 3164–3171; f) A. Bolje, S. Hohloch, D. Urankar, A. Pevc, M. Gazvoda, B. Sarkar, J. Košmrlj, *Organometallics* **2014**, *33*, 2588–2598; g) M. Van der Meer, E. Glais, I. Siewert, B. Sarkar, *Angew. Chem. Int. Ed.* **2015**, *54*, 13792–13795.
- [17] Remarkably, this distortion is compensated when the bond to the peripheral ligands is strong enough as in a pincer palladium complex where a facial tridentate coordination was observed involving both phenyl wingtip groups and the central NHC ligand, presumably stabilized by strong Pd–C bonds. Accordingly, the yaw angle is small, 2.12°, see: N, Stylianides, A. A. Danopoulos, D. Pugh, F. Hancock, A. Zanotti-Gerosa, *Organometallics* **2007**, *26*, 5627–5635.
- [18] a) P. Mathew, A. Neels, M. Albrecht *J. Am. Chem. Soc.* **2008**, *130*, 13534–13535; b) G. Guisado-Barrios, J. Bouffard, B. Donnadiu, G. Bertrand *Angew. Chem. Int. Ed.* **2010**, *49*, 4759–4762; c) J. D. Crowley, A.-L. Lee, K. J. Kilpin, *Aust. J. Chem.* **2011**, *64*, 1118–1132; d) K. F. Donnelly, A. Petronilho, M. Albrecht, *Chem. Commun.* **2013**, *49*, 1145–1159; e) B. Schulze, U. S. Schubert, *Chem. Soc. Rev.*, **2014**, *43*, 2522–2571.
- [19] a) D. Bourissou, O. Guerret, F. P. Gabbai, G. Bertrand, *Chem. Rev.* **2000**, *100*, 39–91; b) W. A. Herrmann, *Angew. Chem. Int. Ed.* **2002**, *41*, 1290–1309; c) F. E. Hahn, M. C.

- Jahnke, *Angew. Chem. Int. Ed.* **2008**, *47*, 3122–3172; d) S. Díez-González, N. Marion, S. P. Nolan, *Chem. Rev.* **2009**, *109*, 3612–3676; e) M. Poyatos, J. A. Mata, E. Peris *Chem. Rev.* **2009**, *109*, 3677–3707; f) M. Melaimi, M. Soleilhavoup, G. Bertrand, *Angew. Chem. Int. Ed.* **2010**, *49*, 8810–8849.
- [20] a) L. Bernet, R. Lalrempuia, W. Ghattas, H. Müller-Bunz, L. Vigara, A. Llobet, M. Albrecht, *Chem. Commun.* **2011**, *47*, 8058–8060; b) A. Petronilho, A. Llobet, M. Albrecht, *Chem. Eur. J.* **2014**, *20*, 15775–15784; c) J. A. Woods, R. Lalrempuia, A. Petronilho, N. D. McDaniel, H. Müller-Bunz, M. Albrecht, S. Bernhard, *Energy Environ. Sci.* **2014**, *7*, 2316–2328; d) A. Petronilho, J. A. Woods, S. Bernhard, M. Albrecht, *Eur. J. Inorg. Chem.* **2014**, 704–708; e) I. Corbucci, A. Petronilho, H. Müller-Bunz, L. Rocchigiani, M. Albrecht, A. Macchioni, *ACS Catal.* **2015**, *5*, 2714–2718.
- [21] a) D. Canseco-Gonzalez, M. Albrecht. *M. Dalton Trans.* **2013**, *42*, 7424–7432; b) B. Bagh, A. M. McKinty, A. J. Lough, D. W. Stephan, *Dalton Trans.* **2014**, *43*, 12842–12850; c) M. Valencia, H. Müller-Bunz, R. A. Gossage, M. Albrecht. *Chem. Commun.* **2016**, *52*, 3344–3347.
- [22] a) D. Canseco-Gonzalez, A. Petronilho, H. Müller-Bunz, K. Ohmatsu, T. Ooi, M. Albrecht, *J. Am. Chem. Soc.* **2013**, *135*, 13193–13203; b) K. F. Donnelly, R. Lalrempuia, H. Müller-Bunz, E. Clot, M. Albrecht, *Organometallics* **2015**, *34*, 858–869; c) G. Kleinhans, G. Guisado-Barrios, D. C. Liles, G. Bertrand, D. I. Bezuidenhout, *Chem. Commun.*, **2016**, *52*, 3504–3507.
- [23] S. Jindabot, K. Teerachanan, P. Thongkam, S. Kiatisevi, T. Khamnaen, P. Phiriyawirut, S. Charoenchaidet, T. Sooksimuang, P. Kongsaree, P. Sangtrirutnugul, *J. Organomet. Chem.* **2014**, *750*, 35–40.
- [24] During our investigations, a close analogue of complex **2** was reported with PF₆[−] as counterion, though the applied procedure required 4 days and afforded complex **2** in 66% yield; see: a) A. Bolje, S. Hohloch, M. V. D. Meer, J. Košmrlj, B. Sarkar, *Chem. Eur. J.* **2015**, *21*, 6756–6764.
- [25] C. Cesarina, R. Mazzoni, H. Müller-Bunz; M. Albrecht, *J. Organomet. Chem.* **2015**, *793*, 256–262.
- [26] a) M. H. S. A. Hamid, P. A. Slatford, J. M. J. Williams, *Adv. Synth. Catal.* **2007**, *349*, 1555–1575; b) G. Guillena, D. J. Ramón, M. Yus, *Angew. Chem., Int. Ed.* **2007**, *46*, 2358–2364; c) T. D. Nixon, M. K. Whittlesey, J. M. J. Williams, *Dalton Trans.* **2009**, 753–762.
- [27] a) N. Yoshimura, I. Moritani, T. Shimamura, S.-I. Murahashi, *J. Am. Chem. Soc.* **1973**, *95*, 3038–3039; b) Y. Shvo, R. M. Laine, *J. Chem. Soc., Chem. Commun.* **1980**, 753–754; c) Bui-The-Khai; C. Concilio, G. Porzi, *J. Organomet. Chem.* **1981**, *208*, 249–251; f) Bui-The-Khai; C. Concilio, G. Porzi, *J. Org. Chem.* **1981**, *46*, 1759–1760; d) C. W. Jung, J. D. Fellmann, P. E. Garrou, *Organometallics* **1983**, *2*, 1042–1044; e) A. Miyazawa, K. Saitou, K. Tanaka, T. M. Gädda, M. Tashiro, G. K. S. Prakash, G. A. Olah, *Tetrahedron Lett.* **2006**, *47*, 1437–1439; f) O. Saidi, A. J. Blacker, M. M. Farah, S. P. Marsden, J. M. J. Williams, *Angew. Chem., Int. Ed.* **2009**, *48*, 7375–7378; g) Z. Yin, H. Zeng, J. Wu, S. Zheng, G. Zhang, *ACS Catal.* **2016**, *6*, 6546–6550.
- [28] a) G. Cami-Kobeci, J. M. J. Williams, *Chem. Commun.*, **2004**, 1072–1073; b) D. Balcells, A. Nova, E. Clot, D. Gnanamgari, R. H. Crabtree, O. Eisenstein, *Organometallics* **2008**, *27*, 2529–2535; c) P. Fristrup, M. Tursky, R. Madsen, *Org. Biomol. Chem.*, **2012**, *10*,

- 2569–2577; d) A. Bartoszewicz, G. González Miera, R. Marcos, P.-O. Norrby, B. Martín-Matute. *ACS Catal.* **2015**, *5*, 3704–3716.
- [29] a) H. Brunner, *Angew. Chem. Int. Ed.* **1999**, *38*, 1194–1208; b) J. Liu, X. Wu, J. A. Iggo, J. Xiao, *Coordination Chemistry Reviews* **2008**, *252*, 782–809.
- [30] a) P. A. Kollman, L. C. Allen, *Chem. Rev.* **1972**, *72*, 283–303; b) L. Brammer, D. Zhao, F. T. Ladido, J. Braddock-Wilking, *Acta Cryst.* **1995**, *B51*, 632–650; c) S. Sabo-Etienne, B. Chaudret, *Coor. Chem. Rev.* **1998**, *178-180*, 381–407.
- [31] The methylene protons appear as an AB pattern in all three complexes between 3.6 and 4.2 ppm, which can be rationalized by the fact that the iridium center is stereogenic.
- [32] E. Akalin, S. Akyüz, *J. Mol. Struct.* **1999**, 482–483, 175–181.
- [33] K. Golcuk, A. Altun, S. Guner, M. Kumru, B. Aktas, *Spectrochim. Acta A-M.* **2004**, *60*, 303–309.
- [34] A. Loris, A. Perosa, M. Selva, P. Tundo, *J. Org. Chem.* **2004**, *69*, 3953–3956.
- [35] a) I. S. Ahuja, P. Rastogi, *J. Inorg. Nucl. Chem.* **1970**, *32*, 2085–2088; b) A. Altun, K. Golcuk, M. Kumru, *Vib. Spectrosc.* **2003**, *33*, 63–74; c) K. Golcuk, A. Altun, M. Kumru, *Spectrochim. Acta A* **2003**, *59*, 1841–1849; d) M. Alvarez, E. Alvarez, M. R. Fructos, J. Urbano, P. J. Perez, *Dalton Trans.* **2016**, *45*, 14628–14633..
- [36] T. Bardakçı, M. Kumru, S. Guner *J. Mol. Struct.* **2013**, *1054–1055*, 76–82.
- [37] T. E. Olalekan, D. R. Beukes, B. Van Brecht, G. M. Watkins, *Journal of Inorganic Chemistry* **2014**, *2014*, Article ID 769573, 10 pages.
- [38] D. S. Glueck, J. Wu, F. J. Hollander, R. G. Bergman, *J. Am. Chem. Soc.* **1991**, *113*, 2041–2054.
- [39] a) S. Arita, T. Koike, Y. Kayaki, T. Ikariya *Organometallics* **2008**, *27*, 2795–2802; b) K.-J. Haack, S. Hashiguchi, A. Fujii, T. Ikariya, R. Noyori, *Angew. Chem., Int. Ed. Engl.* **1997**, *36*, 285–288.
- [40] M. D. Fryzuk, P. A. MacNeil, S. J. Rettig, *J. Am. Chem. Soc.* **1987**, *109*, 2803–2812.
- [41] A. Novak, *Struct. Bonding* **1974**, *72*, 283.
- [42] E. Whalley, *Dev. Appl. Spectrosc.* **1968**, *6*, 277-296.
- [43] R. G. Snyder, J. A. Ibers, *J. Chem. Phys.* **1962**, *36*, 1356–1360.
- [44] R. G. Ball, W. A. G. Graham, D. M. Heinekey, J. K. Hoyano, A. D. McMaster, B. M. Mattson, S. T. Michel, *Inorg. Chem.* **1990**, *29*, 2023–2050.
- [45] a) J. H. Park, K. C. Ko, E. Kim, N. Park, J. H. Ko, D. H. Ryu, T. K. Ahn, J. Y. Lee, S. U. Son, *Org. Lett.* **2012**, *14*, 5502–5505; b) W. Zhao, L. Huang, Y. Guan, W. D. Wulff, *Angew. Chem. Int. Ed. Engl.* **2014**, *53*, 3436–3441; c) P.-P. Zhao, X.-F. Zhou, J.-J. Dai, H.-J. Xu, *J. Org. Biomol. Chem.* **2014**, *12*, 9092–9096; d) C. Su, R. Tandiana, J. Balapanuru, W. Tang, K. Pareek, C. T. Nai, T. Hayashi, K. P. Loh, *J. Am. Chem. Soc.* **2015**, *137*, 685–690; e) D. Niu, S. L. Buchwald, *J. Am. Chem. Soc.* **2015**, *137*, 9716–9721; f) Y. M. A. Yamada, H. Ohta, Y. Yuyama, Y. Uozumi, *Synthesis* **2013**, *45*, 2093–2100; g) C. Segarra, E. Mas-Marzá, J. A. Mata, E. Peris, *Adv. Synth. Catal.* **2011**, *353*, 2078–2084.
- [46] R. C. Clark and J. S. Reid, *Acta Crystallogr.*, **1995**, *A51*, 887–897.

- [47] Oxford Diffraction (2010). *CrysAlisPro* (Version 1.171.34.44). Oxford Diffraction Ltd., Yarnton, Oxfordshire, UK.
- [48] P. Macchi, H. B. Bürgi, A. S. Chimpri, J. Hauser, Z. Gal, *J. Appl. Cryst.* **2011**, *44*, 763–771.
- [49] G. M. Sheldrick, *Acta Crystallogr.*, **2008**, *A64*, 112–122.
- [50] G. M. Sheldrick, *Acta Cryst.* **2015**, *A71*, 3–8.
- [51] G. M. Sheldrick, *Acta Cryst.* **2015**, *C71*, 3–8.
- [52] A. L. Spek, *Acta Cryst.* **2015**, *C71*, 9–18.